PHOTO-ELECTRICAL CONVERSION EFFICIENCY OF DYE SENSITIZED SOLAR CELLS PREPARED FROM MOPANE LEAF CHLOROPHYLL EXTRACT

A MINI THESIS SUBMITTED IN PARTIAL FULFILMENT OF THE REQUIREMENTS FOR THE DEGREE OF MASTER OF SCIENCE (CHEMISTRY)

OF

THE UNIVERSITY OF NAMIBIA

BY

ROCHA TEPHEN KAFFER

201201641

APRIL 2020

MAIN SUPERVISOR: Prof. Likius Shipwiisho Daniel (University of Namibia)

CO-SUPERVISOR: Dr. Kalengay Mbela (University of Namibia)

ABSTRACT

In times of fossil fuel shortage, increasing crude oil prices, as well as rejection of conventional energy sources (e.g. coal or nuclear power plants), sustainable energy forms become more and more the focus of attention. One of several offered solutions is to develop a photovoltaic device (solar cells), since solar energy is abundant. Especially, Namibia receives solar radiation of 5.8 to 6.4 KWh per square meter per day – one of the highest in the world. With 8 to 11 average hours of sunshine per day throughout the year, this offers fantastic potential for solar energy, both photovoltaics and solar thermal. Dye Sensitized Solar Cell (DSSC) which is presented here is a thin film cell. Manufacturing of DSSCs is simple, mostly low cost, and incorporate environmentally friendly materials. They have a good efficiency (about 10-14 %) even under low flux of sunlight. However, a major drawback is the temperature sensitivity of the liquid electrolyte. Hence, this study presents the ongoing research to improve the electrolyte's performance by using natural dye. A transparent conductive oxide (TCO) film of Fluorine - doped Tin Oxide (FTO) was used as an anode. In this research, chlorophyll extracted from *Colophospermum Mopane* leaves using methanol was employed as the dye for TiO_2-based DSSC. TiO_2 precursor solution prepared by Molecular precursor method (MPM) was spin-coated on top of Fluorine- Doped Tin Oxide (FTO) conductive glass and calcined at 420˚C for 20 min to act as an anode electrode. The cathode electrode was a supportive glass substrate coated with a layer TiO_2 paste (Degussa P25) followed by graphene layer obtained from charcoals sold in Namibian markets. The anode electrode was then immersed in the dye for 20 min, to make the TiO_2-chlorophyll thin film. An iodide/triiodide solution was used as the electrolyte. Both electrodes were then pressed together and sealed so that the cell does not leak to make TiO_2-Graphene-Chlorophyll-TiO_2 sandwich structure based DSSC.

An external load was supplied when sunlight shine on the anode of the cell. The photovoltaic performance of this assembled DSSC was then measured using a multi-meter employing eDAG Potentiostat R466 and Echem software under direct sunlight illumination. Furthermore, the assembled cell efficiency was determined by plotting an IV-curve. The current and voltage values for the cell were 157.4 µA and 510 mV respectively. The resistance of the assembled DSSC was 0.931 Ω. Open circuit voltage 287.1 mV, short circuit current 170.8 µA, fill factor 33.5 %, with an efficiency of 0.37 % was obtained. The cell was tested under direct sunlight illumination having a power input of 4.5 mW, on the solar cell area of 7.8 cm^2. These results were supported by the UV/Vis analysis showing that both chlorophyll and TiO_2 do absorb photons in the wide range of 300 nm to 1000nm. A wide absorption range means that the cell can absorb in the visible and IR light which make up about 90% of the solar spectrum. Large active surface area exposure for the TiO_2, enabled more dye and electrolyte to be stored inside the material so that photon adsorptions from solar energy became more effective, resulting in higher efficiency. Despite the small efficiency, this work demonstrated the opportunities of Chlorophyll and TiO_2 to be applied as a DSSC.

TABLE OF CONTENTS

LIST OF TABLES

LIST OF FIGURES

LIST OF ABBREVIATIONS AND/OR ACRONYMS

DSSCs	Dye Sensitized Solar Cells
MPM	Molecular Precursor Method
$S_{titania}$	Titania Precursor
E_g	Band gap energy
eV	electron volts
HOMO	Highest occupied molecular orbital
LUMO	Lowest unoccupied molecular orbital
UV	Ultraviolet
Vis	Visible
WE	Working Electrode
CE	Counter Electrode
CARBO Charcoal (activated)	CARBO-chac
FTO	Fluorine-doped tin oxide
TiO_2	Titanium dioxide (Titania)
EG	Ethylene glycol
PCE	Photo conversion efficiency

ACKNOWLEDGEMENTS

First of all, I would like to thank the almighty Father for giving another opportunity, wisdom and strength to pull through this journey towards achieving my goal. I also wish to extend my sincere gratitude to my supervisor, Dr. Likius Shipwiisho Daniel (UNAM's Faculty of Science, Chemistry and Biochemistry Department), for his ardent support and academic guidance throughout the course of this study. It is highly appreciated. Also, Dr. Kalengay Mbela, (UNAM's Rundu Campus), for his contribution towards the success of my studies. It is duly noted.

Next, I also want to acknowledge the University of Namibia, Department of Chemistry and Biochemistry, the Center for Postgraduate Studies for rendering my study with the necessary equipment, reagents and a laboratory during my studies though there were shortcomings.

Last but not the least, my sincere gratitude also goes to Ms. Kalipi, Mr. Naihmwaka, Ms. Endjala, friends and family for their effortless support, words of encouragement and faith that they instill in me.

DEDICATION

This work is dedicated to my grandmother, Magdalena Goliath, my sister, Venessa Kaffer, my niece, Precious Kaffer, and my uncle, Salmon Patrick Kaffer.

DECLARATIONS

I, **Rocha Tephen Kaffer**, hereby declare that this study is my own work and is a true reflection of my research, and that this work, or any part thereof has not been submitted for a degree at any other institution.

……..……	……	…….
Name of Student	Signature	Date

CHAPTER 1: INTRODUCTION

1.1 Background of the study

Over billions of years, the earth has been converting sunlight into energy via photosynthesis. Sunlight is the most abundant and sustainable energy source that is free. The Earth receives energy from the sun at the rate of ~1.2×10^{17} J s^{-1} [1]. This exceeded the yearly worldwide energy consumption rate of ~1.5×10^{13} J s^{-1}[1]. Therefore, it is a challenge to devise an approach for the effective capture and storage of solar energy for our consumption since fossil fuels such as oil and gas will be depleted in years to come [2]. In order to imitate the photosynthesis process, Grätzel has developed dye-sensitized solar cells (DSSCs) based on the similar working mechanism [3]. Figure 1 shows the typical DSSC. Nevertheless, one main difference between photosynthesis of plants and DSSCs is that the energy can be stored in plants for later use but DSSC is unable to store energy. Ever since the birth of DSSCs, they have become the spotlight of attention among scientists and researchers around the world as they are much cheaper, easier to fabricate, and more environmentally friendly when compared with conventional silicon solar cells [4].

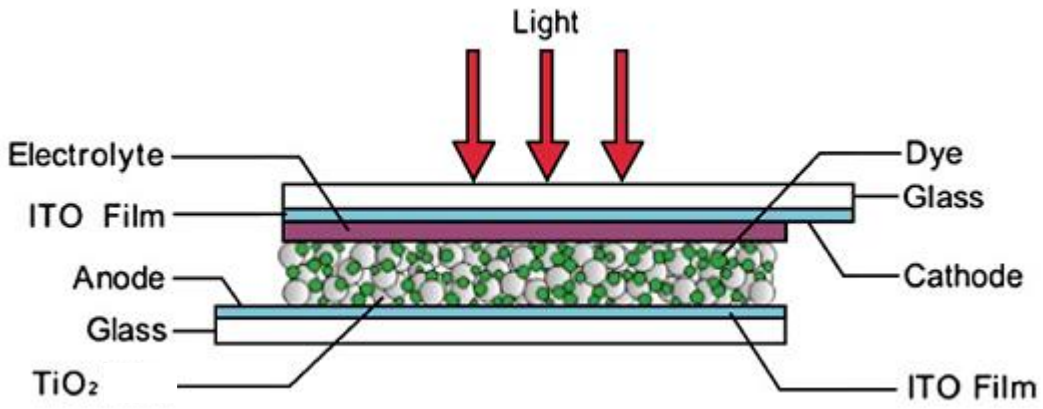

Figure 1 Structure of photosynthetic pigments-sensitized TiO_2 solar cell.

A DSSC is an electrochemical device that comprises a transparent-conducting oxide (TCO) glass over which is deposited a semiconductor. The semiconductor is soaked in a dye solution. An electrolyte with reduction-oxidation (redox) mediator and cathode are the other remaining components. The fluorine-doped tin oxide (FTO)/semiconductor/dye assembly is referred to as photoanode. Indium-doped tin oxide (ITO) and FTO are two TCOs used commonly in DSSCs. Titanium dioxide (TiO_2) is one of the popular semiconductors used for DSSC since it is cheap, non-toxic, and possesses a large band gap [5]. TiO_2 is deposited on the TCO substrate in the form of TiO_2 nanoporous particle network to increase the coverage area for the sensitizing dye. The cathode is made up of another TCO on top of which platinum is deposited. Carbon and conducting polymers can also be employed as counter electrodes. If a gel polymer electrolyte is used, it is sandwiched between the photoanode and cathode. The dye, on the other hand, can be categorized into two groups: synthetic and natural. The most frequently used synthetic dyes are the ruthenium (Ru)-based dyes but they are not environmentally friendly since Ru is a heavy metal [6]. Such dyes are also very expensive due to the scarcity of Ru. By contrast, natural dyes are readily available and thus cheap besides being non-toxic, environmentally friendly, biodegradable, easily extracted as well as can be used without any purification. Since DSSC mimics the photosynthesis of green plants, therefore chlorophyll can also function as photosensitizer for DSSC. In fact, report on chlorophyll as photosensitizer on zinc oxide (ZnO) semiconductor was first published by Tributsch in 1972 [7].

Today, several natural dyes have been utilized as sensitizers for DSSCs. El-Agez et al. [8,9] studied natural dyes extracted from fresh and dried plant leaves and found that spinach oleracea extract has a better performance after drying where the efficiency of

the cell prepared with TiO_2 thin film layer reached 0.29%. Plant seeds have been used as sensitizers and it was found that DSSCs sensitized with the extracts of onion, rapa, and Eruca sativa seeds have efficiencies of 0.875%, 0.86%, and 0.725%, respectively [10]. In 2008, red Sicilian orange juice dye was used as a sensitizer and a conversion efficiency of 0.66% was reported [10]. Rosella was used as a sensitizer for DSSCs with efficiency of 0.70% [11]. Roy et al. reported that DSSCs sensitized with Rose Bengal dye can have conversion efficiency of 2.09% [12]. The modified structure of coumarin derivative dye was proposed by Wang et al. [13] which provided an efficiency of 7.6%. J. Etula and R. Ahmadian [15] studied the structure and the concentration of anthocyanins, respectively, in several natural dyes used as sensitizers for DSSCs. It was hypothesized, that natural dyes with higher anthocyanin concentration, such as those extracted from blueberry and black raspberry, have higher fill factors and efficiency. Chlorophyll (A) structure in Punica granatum peel extract gave a solar cell with 1.86% conversion efficiency [16]. In general, natural pigments, such as anthocyanins, carotenoids, and chlorophylls, have several advantages over rare metal complexes for DSSC sensitization. It has been shown that chlorophyll has good potential to serve as photosensitizer in dye-sensitized solar cells. Moreover, they are cheap, non-toxic, biodegradable, easily found, and easy to use as sensitizer. Although the efficiency is still considerably low with highest efficiency to date being only 4.6% from DSSC with *U. pinnatifida* chlorophyll C_2, there remains the possibility and room for improvement to further enhance the performance and improve stability of chlorophyll-sensitized DSSCs for practical applications. In this thesis, the extracts of chlorophyll from the *Colophospermum Mopane* leaves (Mopane leaves) is used as sensitizer for TiO_2-Graphene-Chlorophyll-TiO_2 Sandwich Structure as DSSC. The extracts are characterized by UV-Vis absorption spectroscopy. TiO_2 thin film is used

as a semiconducting material. The photovoltaic tests of DSSC are carried out under an incident irradiation from direct sunlight.

There are quite number of ways of fabricating thin films. These methods are classified as physical and chemical. For the purpose of this study, the chemical method of fabrication, namely Molecular Precursor Method was used. Nagai and Sato [17] define Molecular Precursor Method (MPM) as a wet chemical process for the creation of thin films of various metal oxides, this includes titanium dioxide or calcium phosphate compounds. The precursor thin films produced by this method requires heat treatment to remove any organic ligands in the precursor solution. MPM has an advantage of excellent stability, homogeneity, miscibility, and coating thus forming metal complex coating with those characteristics [18]. MPM forms well developed thin films [17]. Furthermore, Nagai and Sato [17] state that the crystal size of the oxide particles in the thin films fabricated by this method is normally smaller than those fabricated via the conventional sol-gel method.

MPM involves reacting titanium tetraisopropoxide with ethylenediaminetetraacetic acid (EDTA), in dibutylamine solution and hydrogen peroxide [18]. The resultant precursor solution is then spin coated on glass substrates to form precursor composite thin films. Therefore, after the fabrication of a DSSC using MPM, the evaluation the its performance, the Overall Energy Conversion Efficiency is considered. Other required parameters are J_{sc} (short-circuit current density), I_{sc} (short-circuit current), V_{oc} (open-circuit-voltage), and FF (fill-factor). The short circuit-current is the current across the solar cell when voltage is zero (i.e., when the solar cell is short circuited). Open circuit voltage is the maximum voltage available from a solar cell, which is obtain from splitting hole and electron Fermi levels. Fill factor is described the quality of the solar cell, calculated as the rate of maximum power from the actual solar cell

per maximum power from an ideal solar cell. Efficiency is described as the ratio of energy output from the solar cell to input energy from the sun.

1.2 Statement of the problem

In Namibia, the *Colophospermum Mopane* remains an underutilized plant with little information available about its uses. This research on the photo-electrical conversion efficiency of DSSC prepared from mopane leaf chlorophyll extract is important, in order to make the local people, and the whole world at large, aware about the potential use of *Colophospermum Mopane* leaf chlorophyll extract as a dye in DSSC.

1.3 Objectives of the study

The objectives of the study were:

(a) To construct TiO_2-CARBO-chac as a counter electrode.

(b) To create TiO_2-Chlorophyll thin film.

(c) To assemble TiO_2-CARBO-chac-TiO_2-Chlorophyll sandwich based DSSC.

(d) To test the photo - electrical conversion efficiency of the assembled DSSC.

1.4 Significance of the study

This study provides information on the use of TiO_2-CARBO-chac-TiO_2-Chlorophyll sandwich based DSSC, which has the potential to improve the overall photo-electrical conversion efficiency for DSSCs. In addition, the TiO_2-CARBO-chac aids in the absorption of photons in the visible and infrared regions. In this case CARBO-chac shifts the photo-responsive threshold frequency of TiO_2 into the visible region. Furthermore, it uses chlorophyll that was harvested from an indigenous plant *Colophospermum Mopane*. *Colophospermum Mopane* grows in the northern parts of Namibia.

CHAPTER 2: LITERATURE REVIEW

2.1 Overview

The modern version of a Dye Sensitized Solar Cell, also known as the Grätzel cell, was initially co-invented in 1988 by Brian O'Regan and Michael Grätzel at University of California, Berkeley and this work was later developed by the aforementioned scientists at the École Polytechnique Fédérale de Lausanne until the publication of the first high efficient DSSCs in 1991 [19]. Research has been done to enhance the efficiency of Grätzel cell using environmentally friendly and affordable materials [19]. There is a need to shift the absorption threshold of the UV-region response of TiO_2 into the visible region which can be achieved by doping TiO_2 with dye sensitizers [18]. Chlorophyll which aids in the absorption of sunlight by plants can also be used as a natural dye [20,21].

Solar cells are devices which use photo-voltaic effects to convert solar energy into electrical energy, as shown in figure 2 [22]. Semiconductor material produce chemical energy by separating photon and electron known as the potential energy difference. Solar cells are classified into three groups based on the material they are made of, namely first-generation solar cells (crystalline silicon solar cells), second generation solar cells (thin film solar cells) and third generation solar cells (organic solar cells). Dye-sensitized solar cells (DSSCs) are low-cost solar cells belonging to a group of thin film solar cells (2^{nd} generation solar cells) [23]. DSSCs are based on a semiconductor formed between a photo-sensitized anode and an electrolyte [23]. A modern DSSC is composed of a layer of titanium dioxide (Titania or TiO_2) nanoparticles, covered with a dye that absorbs sunlight such as chlorophyll [22,23].

The TiO_2 is immersed in an electrolyte solution, above a transparent conductive oxide (TCO) films-based electrode.

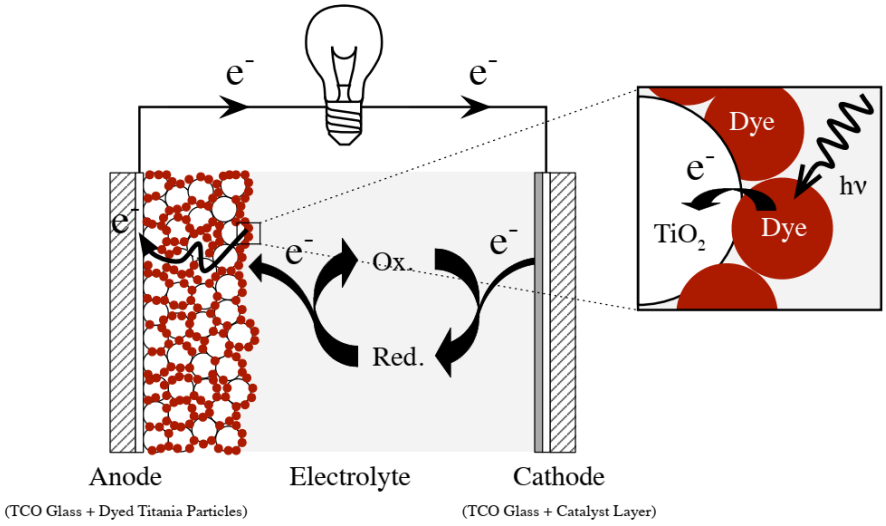

Figure 2 Photovoltaic conversion of sunlight in DSSC, excitation of dye by a photon, electron injected into titania, which later flow through the bulb [22].

Titanium dioxide is a naturally occurring oxide of titanium. In nature it occurs as three forms of titania namely ilmenite (brookite), rutile, and anatase (figure 3). Titanium dioxide is highly stable, highly reactive, non-toxic and cost effective [18]. It has a variety of applications in paints, sunscreen, and food coloring [18]. Titanium dioxide is a semiconductor with band gap (E_g) of 3.0 – 3.2 eV [24]. Due to this wide band gap, it requires lot of energy to promote or excite electrons in the valence band to conduction band of titanium dioxide [25]. Furthermore, titanium dioxide is limited to absorbance of ultraviolet (UV) light which only accounts for 3 – 5 % of solar radiation as illustrated in figure 3 below [18,24]. As a result, research has been extensively done on titanium dioxide to tune its threshold energy to make use of visible-light by doping it with various materials such as dye sensitizers, non-metals, and transition nano-noble metals. Visible light constitutes approximately 40 % of solar radiation (figure 4) [18].

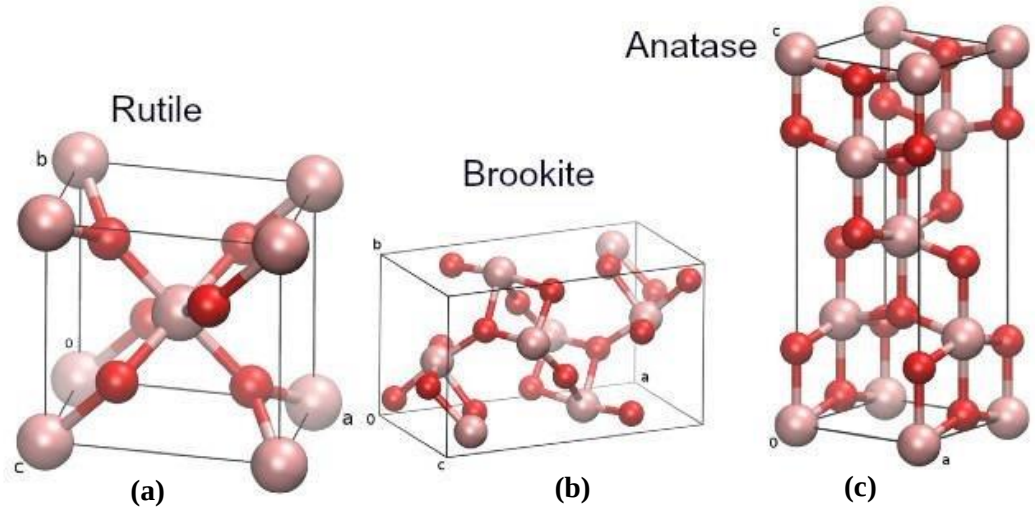

Figure 3 The three phases of titanium dioxide (a) rutile, (b) brookite or ilmenite, and (c) Anatase [18].

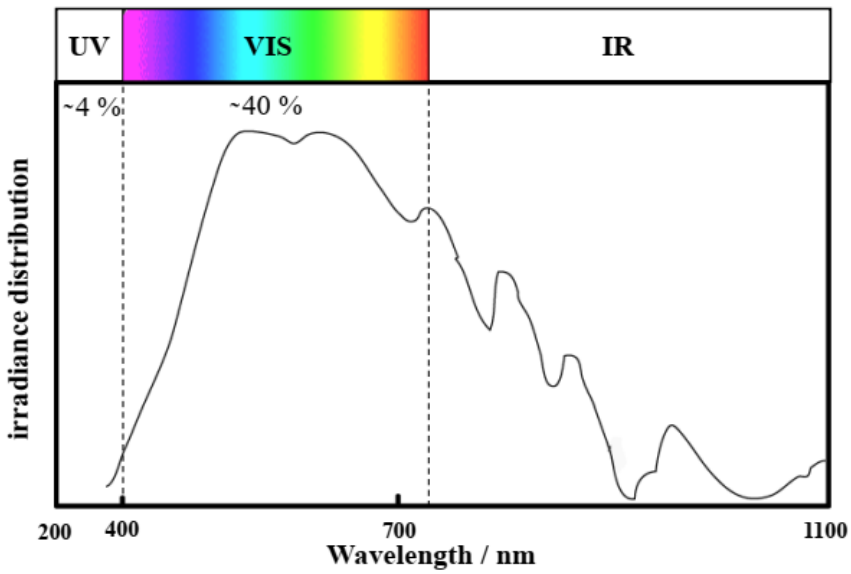

Figure 4 Standard solar spectral irradiance (AM 1.5 global) [18].

Graphene has been extensively studied in numerous solar cell applications due to its good mechanical strength and remarkable charge transport properties [26]. Activated charcoal's extraordinary explicit surface area allows active catalytic sites for charge storage and electrochemical reactions, maintaining a multi-edge porous morphology [27]. However, it is limited by low substrate adhesion and comparatively low

conductivity, resulting in large internal impedance [27]. Coupling activated carbon with other materials such as titanium dioxide blocking layer could enhance its low conductivity and capacitance as a counter electrode (CE) [26].

Chlorophyll is a natural pigment that aids photosynthesis in a plant [20]. Figure 5 illustrates the chemical structures of chlorophyll a and chlorophyll b. Since it absorbs blue and red light it is employed in DSSCs as sensitizers [21]. In addition, chlorophyll absorbs visible light and near infrared light, as shown in figure 5 below [28]. Chlorophyll can be easily obtained from *Colophospermum Mopane* leaves, it is biodegradable, and environmentally friendly thus considered for this research (figure 6).

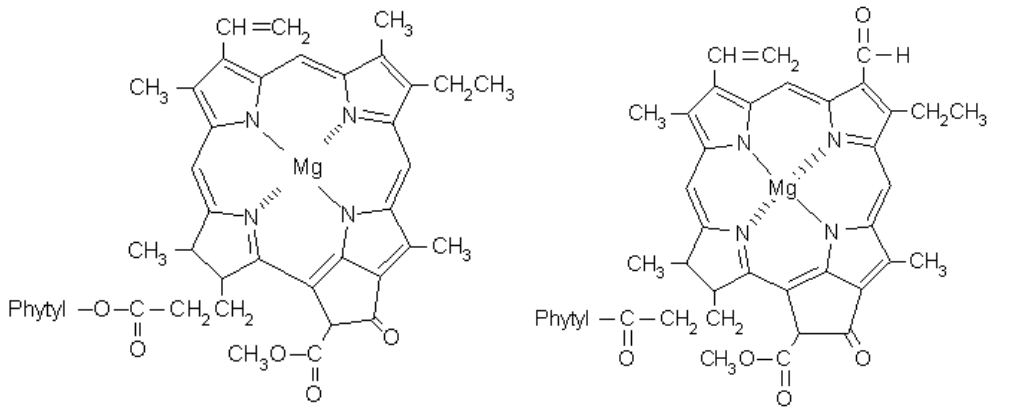

(a) **(b)**

Figure 5 Chemical structure of (a) chlorophyll a, and (b) chlorophyll b [20].

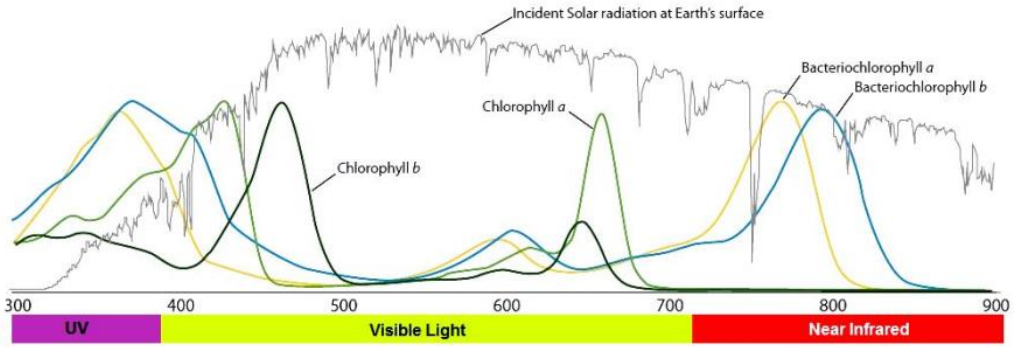

Figure 6 Absorption spectrum of solar radiation and chlorophyll absorbance [28].

2.2 Dye Sensitize Solar Cells (DSSCs)

2.2.1 Overview

DSSCs have been proposed as an alternative to 1st generation crystalline silicon solar cells. These cells are cost-effective, highly efficient photovoltaic energy converters [29]. The sensitized dye absorbs inbound sunlight and excite electrons from the highest occupied molecular orbital (HOMO) to the lowest unoccupied molecular orbital (LUMO) [30]. The electrons which are knocked lose are then injected into the photoanode, which infiltrate through the photoanode and reach the CE [30]. The electrolyte revitalizes the oxidized dye molecules through reducing the species in the electrolyte [29]. The shape and the structure of the photoanode material are the key factors in photoelectric conversion efficiency [30]. Titanium dioxide (TiO_2) is widely used as photoanode material in DSSCs [19-30]. The adsorption of dye on TiO_2 surface slightly changes the energy levels of the dye [30].

2.2.2 Components of DSSCs

DSSCs are made up of a working electrode (WE), sensitizer (dye), electrolyte, and counter electrode (CE). The dye molecule is applied on the working electrode and

further attached to the counter electrode saturated with a thin layer of electrolyte, a sealant is used to prevent the loss of an electrolyte.

Light absorption, electron injection, transportation of carrier, and collection of current are the principles on which DSSC operate [19]. The phases of the photovoltaic performance of DSSC are, as outlined by Sharma et al. [19], illustrated in figure 7:

1. Photon absorption by a dye sensitizer, and as such, electrons are excited from ground state to excited state of the sensitizer, where absorption takes place which is mostly in the ultraviolet-vis (UV-vis) and near infrared region (NIR) regions analogous to 1.72 eV photon energy.
2. The excited electrons are then injected into the conduction band of nanoporous TiO_2 electrode in nanosecond timing, this layer lies underneath the excited state of the dye, photons from the UV region are absorbed by TiO_2 in infinitesimal amounts. The dye is oxidized because of this phenomenon.
3. When electrons are injected, they are transported between TiO_2 nanoparticles and the TCO, where they diffuse towards it. Finally, electrons flow through the external circuit to the CE.
4. Reduction of I^-_3 species to I^- occur at the CE, as a result dye restoration of its ground state happens as it receives electrons from I^- species (redox mediator), and I^- species are oxidized to I^-_3.
5. The I^-_3 species scatters to the CE and reduces to I^- species.

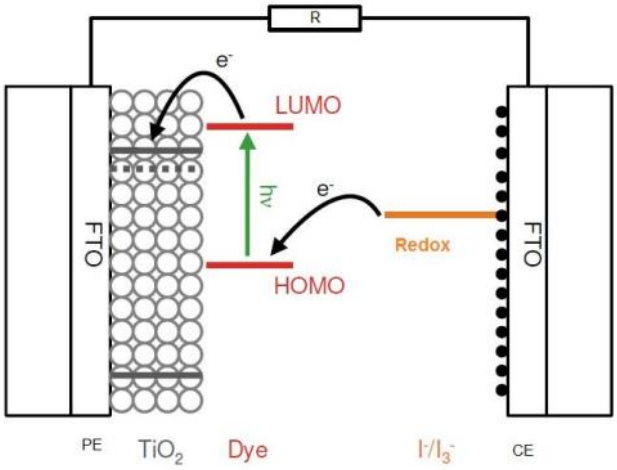

Figure 7 Basic components DSSC namely the working electrodes, dye sensitizer, electrolyte, and the counter electrode [28].

2.2.3 Sensitized Dye Adsorbent

The anode is made of TiO_2 nanoparticles that are spread out in a thin layer on a transparent conductive glass electrode. These nanoparticles provide a large surface area for the dye molecules to attach, and thus provide an electron pathway for the generation of electric current. The purpose of these nanoparticles is to absorb the sensitizer on its surface. Figure 8 demonstrates the adsorption of dye sensitizer on the titania surface.

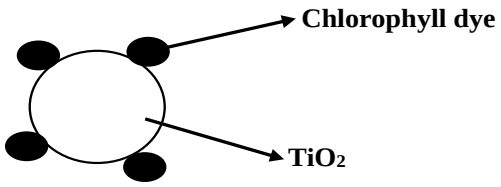

Figure 8 Adsorption of chlorophyll dye sensitizer onto TiO_2 (titania surface).

2.2.4 Transparent and Conductive Substrate

The deposition of the semiconductor and a catalyst occurs due to the conductive transparent materials for DSSCs, which act as current collectors (figure 7) [19]. These

materials are characterized by transparency, efficient charge transfer and reduced energy loss [19]. The conductive substrates for DSSCs are normally the indium-doped tin oxide (ITO) and fluorine-doped tin oxide (FTO). Herein, FTO glass substrate was used for the TiO_2-Graphene-Chlorophyll-TiO_2 sandwich based DSSC. ITO glass substrate has a transmittance of > 80% with sheet resistance of 18 Ω/cm^2, whereas FTO glass substrate has ~ 75% transmittance in the visible region and 8.5 Ω/cm^2 sheet resistance [19].

2.2.5 The Working Electrode (WE)

Working electrode is made up of a semiconductor (n-type) and metal or non-metal (p-type) material on TCO glass substrate. TiO_2 is commonly used as a semiconductor (n-type) due to its non-toxicity, relative availability and easy access. However, TiO_2 does not absorb visible light so it is sensitized with a dye molecule. In order to sensitized TiO_2, the film is soaked in a photosensitizer which binds covalently to the TiO_2 surface [19]. Large surface area and highly porous structure allows maximum absorption of the sensitizer onto the nanocrystalline TiO_2 layer, and in turn enhances the light absorption capacity of the n-type semiconductor [19].

2.2.6 The Dye sensitizer

Incident light is absorbed by the dye sensitizer in the DSSC. For a material to be used as a photosensitizer, it should possess the following photophysical and electrochemical properties, as outlined by Sharma et al. [19]:

1. The dye ought to be luminescent.
2. The dye should absorb both ultraviolet-visible and near-infrared light.

3. The dye HOMO energy level must be far from the conduction band of TiO_2, and the LUMO energy level be near that of TiO_2, but be higher in correlation to the conduction band potential of TiO_2.
4. HOMO energy level of the redox electrolyte should be higher than that of the dye.
5. The dye should have a hydrophobic boundary to boost the stability of the cell, if not, water-induced distortion may occur from the TiO_2 film thus reducing the stability of the cell.

Dye sensitizers are grouped into two classes, namely inorganic dye (which includes metal complex) and organic dye (this includes natural and synthetic organic dye) [21].

a) Inorganic dye

Ruthenium (Ru) complex dye is mostly used for DSSC studies. Though it produces high efficiencies it is very expensive and relatively challenging to synthesize [21]. Ru complexes are categorized as carboxylate polypyridyl Ru dyes, phosphonate Ru dye, and polynuclear bipyridyl Ru dyes [21]. These complexes are N3 dye, N719 dye, and N749 dye (black dye). The N3 dye absorbs up to 800 nm radiation, and the black dye up to 860 nm radiation [21]. Figure 9 below shows the chemical structure of Ru complexes.

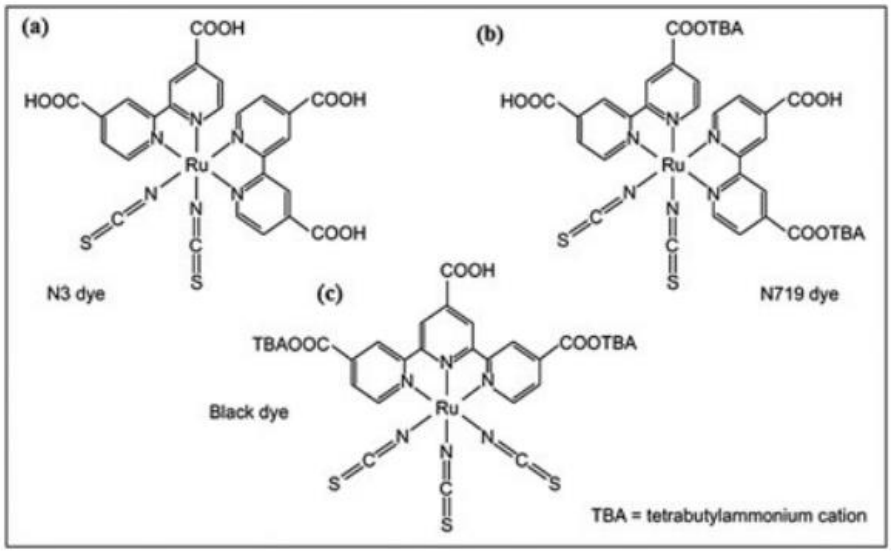

Figure 9 Chemical structure of Ru complexes (a) N3 dye, (b) N719 dye, and (c) N749 dye [21].

b) Organic dye

DSSCs principles operate in similar manner as photosynthesis thus scientists initially considered natural dyes as photosensitizers [21]. Organic dye contains carboxyl, or hydroxyl groups which have the ability of chelating to Ti^{4+} species on the TiO_2 surface [31]. This binding ability is demonstrated in figure 10 below.

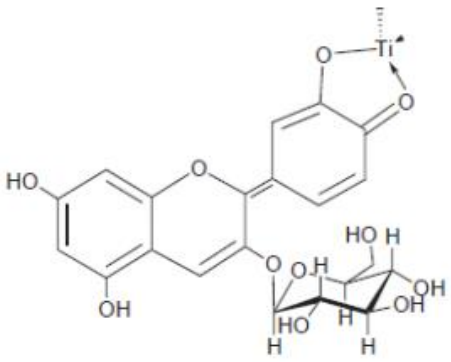

Figure 10 Cyanin-Ti^{4+} complex formed via the adsorption of organic cyanine dye solution onto the TiO_2 surface [31].

Most plants, and flowers have different pigments which are used as sensitizers, chlorophyll being one of them. Chlorophyll absorbs photons from solar radiation, and reflects green wavelength, thus the green color it possesses [31]. It has prominent absorption peaks at 420 nm and 600 nm wavelengths (visible light region) [8-10, 14]. Figure 11 shows the absorption spectrum of chlorophyll dye solution as reported by Alhamed and co-workers [31].

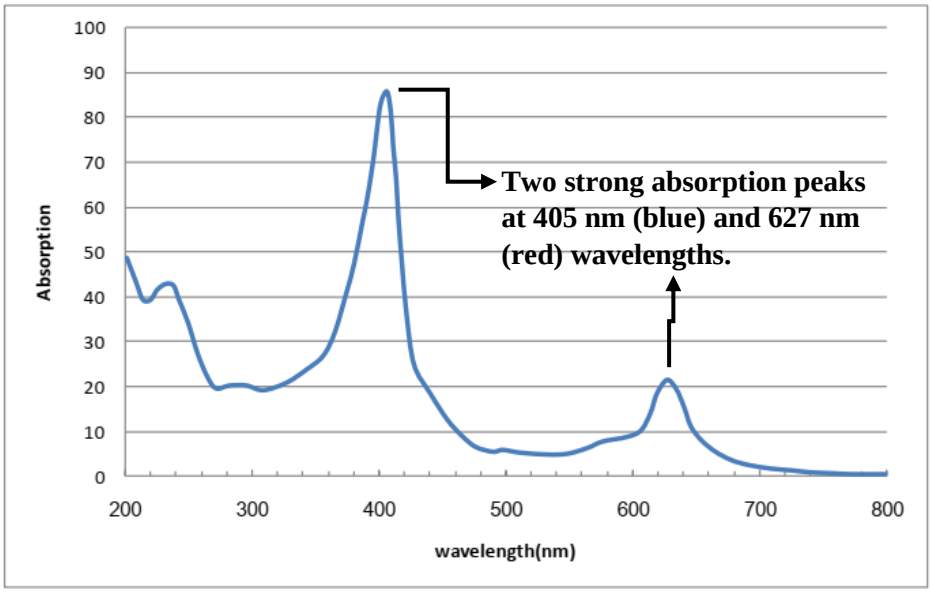

Figure 11 Absorption spectrum of Chlorophyll dye solution, shows strong absorption peaks at 405 nm and 627 nm wavelengths [31].

Chlorophyll absorbs visible light thus it is possible for it to be used in DSSCs as the main aim of DSSCs is to enhance the photocatalytic and photoluminescence of the titanium dioxide nanoparticles.

2.2.7 Electrolyte

Redox couple, solvent, additives, ionic liquids, and cations are the main constituents of an electrolyte [19]. An electrolyte can have one of the following species (redox coupling) namely I^-/I^-_3, Br^-/Br^-_2, SCN^-/SCN_2, and Co (II)/Co (III) [19].

An electrolyte should have the following features [19]:

1. Effective regeneration of the oxidized dye by the redox coupling.
2. Long-term chemical, thermal, and electrochemical stability.
3. The dye must be non-corrosive with the components of DSSC.
4. Must allow fast diffusion of charge carriers, enhance conductivity, and create efficient contact between the WE and CE.
5. The electrolyte absorption spectra and the dye absorption spectra must not overlap.

The most commonly used redox coupling, I^-/I^-_3, corrodes glass/TiO_2/Pt, is highly volatile, and causes photodegradation and dye desorption, associated with reduced long-term stability [19]. Though there are many plausible substitutes for this redox coupling, they also face tremendous limitations compared to I^-/I^-_3 coupling.

2.2.8 Counter Electrode (CE)

In DSSCs counter electrode is mainly filled with platinum (Pt) or carbon (C). The reduction of I^-/I^-_3 species is initiated at the CE and thus collects holes from the hole transport materials (HTMs) [19]. Higher efficiencies are achieved with Pt-CE, but due to its higher cost and rarity, the search for its replacement were considered. These alternatives have been tested in several studies, though, lower efficiencies were reported for such alternatives [31].

2.3 Outlook on DSSCs studies

This section discusses the studies reported for DSSCs using chlorophyll as a natural dye, and activated charcoal or any related carbonaceous material as counter electrodes.

Arof and Ping [27] summarized the performance of some DSSCs using chlorophyll as a dye described by researchers globally (**Table 1**). These researches were done under

intensity of 100 mW cm^{-2} illumination of the chlorophyll photosensitized DSSCs unless specified otherwise.

Table 1 Summarized performance of some DSSCs using chlorophyll photosensitizer as reported by Arof and Ping [27].

	Photoanode	Electrolyte	Counter electrode	J_{sc} (mA cm^{-2})	V_{oc} (V)	*FF*	η (%)
Anethum graveolens leaves (fresh)	TiO_2/FTO	I^-/I_3^- LE	Pt/FTO	0.965	0.579	0.400	0.220
Anethum graveolens leaves (dried)	TiO_2/FTO	I^-/I_3^- LE	Pt/FTO	0.454	0.562	0.320	0.080
Arugula leaves (fresh)	TiO_2/FTO	I^-/I_3^- LE	Pt/FTO	0.788	0.599	0.420	0.200
Arugula leaves (dried)	TiO_2/FTO	I^-/I_3^- LE	Pt/FTO	0.713	0.594	0.430	0.180
Parsley leaves (fresh)	TiO_2/FTO	I^-/I_3^- LE	Pt/FTO	0.535	0.445	0.340	0.070
Parsley leaves (dried)	TiO_2/FTO	I^-/I_3^- LE	Pt/FTO	0.448	0.553	0.400	0.090
Bougainvillea spectabilis flower	TiO_2/ITO	I^-/I_3^- GPE	PEDOT/FTO	1.110	0.500	0.586	0.325
Amaranthus caudatus flower	TiO_2/ITO	I^-/I_3^- GPE	PEDOT/FTO	1.820	0.550	0.610	0.610
Cordyline fruticosa leaves	TiO_2	Not stated	Not stated	1.300	0.616	0.602	0.500
Pawpaw leaves	TiO_2/FTO	LE	Not stated	0.649	0.504	0.605	0.200
Pomegranate leaves	TiO_2/ITO	I^-/I_3^- LE	Pt/FTO	2.050	0.560	0.520	0.597
Platanus orientalis L. (Chinar leaves)	TiO_2/ITO	I^-/I_3^- LE	Pt/ITO	0.012	0.468	0.004	0.550
Shiso leaves	TiO_2/FTO	p-CuI	-	3.520	0.432	0.390	0.590
Bougainvillea leaves	Au/TiO_2/FTO	I^-/I_3^- LE	Pt/FTO	3.230	0.500	0.410	0.618
Ocimum Gratissimum (scent leaves)	TiO_2/FTO	I^-/I_3^- LE	Pt/FTO	0.044	0.466	0.400	0.021
Spinach oleracea	TiO_2/ITO	I^-/I_3^- LE	Pt/ITO	0.467	0.550	0.510	0.131
Spinach oleracea (fresh)	TiO_2/FTO	I^-/I_3^- LE	Pt/FTO	0.332	0.590	0.420	0.080
Spinach oleracea (dried)	TiO_2/FTO	I^-/I_3^- LE	Pt/FTO	1.110	0.583	0.460	0.290
	ZnO/FTO	I^-/I_3^- LE	Pt/FTO	0.123	0.226	0.200	0.008
Red spinach leaves	TiO_2/ITO	I^-/I_3^- LE	C/FTO	1.000	0.505	0.578	0.583
	TiO_2/ITO	I^-/I_3^- LE	C/FTO	0.700	0.559	0.455	0.357
	TiO_2/ITO	I^-/I_3^- LE	C/FTO	0.500	0.750	0.394	0.296
Green spinach leaves	ZnO/ITO	I^-/I_3^- LE	C/ITO	0.052	0.590	0.530	0.016

	Photoanode	Electrolyte	Counter electrode	J_{sc} (mA cm^{-2})	V_{oc} (V)	*FF*	η (%)
Papaya leaves	TiO_2/FTO	I^-/I_3^- LE	Pt/FTO	0.360	0.325	0.560	0.070
	TiO_2/ITO	I^-/I_3^- LE	C/FTO	0.060 mA	0.394	0.250	-
Jatropha leaves	TiO_2/ITO	I^-/I_3^- LE	C/FTO	0.042 mA	0.350	0.250	-
Ipomoea leaves extract	TiO_2/ITO	I^-/I_3^- LE	Pt/ITO	0.850	0.495	0.536	0.233
	TiO_2/ITO	I^-/I_3^- LE	Pt/ITO	0.914	0.540	0.563	0.278
	TiO_2/ITO	I^-/I_3^- LE	Pt/ITO	0.825	0.533	0.548	0.259
	TiO_2/ITO	I^-/I_3^- LE	Pt/ITO	1.120	0.565	0.592	0.318
	TiO_2/ITO	I^-/I_3^- LE	Pt/ITO	0.982	0.543	0.564	0.292
	TiO_2/ITO	I^-/I_3^- LE	Pt/ITO	0.915	0.510	0.552	0.253
Azadirachta indica (Neem) leaves	TiO_2/FTO	I^-/I_3^- LE	C/FTO	0.430	0.404	0.401	0.720
	TiO_2/FTO	I^-/I_3^- LE	Pt/FTO	0.230	0.467	0.392	0.050
Ziziphus jujuba leaves (dried)	TiO_2/FTO	I^-/I_3^- LE	Pt/FTO	3.180	0.652	0.519	1.077
Basil leaves (dried)	TiO_2/FTO	I^-/I_3^- LE	Pt/FTO	1.398	0.581	0.499	0.409
Basil flower	TiO_2/FTO	I^-/I_3^- LE	Pt/FTO	1.120	0.600	0.400	0.270
Mint flower	TiO_2/FTO	I^-/I_3^- LE	Pt/FTO	0.450	0.560	0.380	0.090
Mint leaves (dried)	TiO_2/FTO	I^-/I_3^- LE	Pt/FTO	0.980	0.579	0.400	0.227
Lemon leaves[a]	TiO_2/FTO	I^-/I_3^- LE	C/FTO	1.080	0.592	0.100	0.036
Morula leaves[a]	TiO_2/FTO	I^-/I_3^- LE	C/FTO	0.059	0.472	0.050	0.001
Fig leaves (dried)	TiO_2/FTO	I^-/I_3^- LE	Pt/FTO	2.091	0.596	0.515	0.642
Berry leaves (dried)	TiO_2/FTO	I^-/I_3^- LE	Pt/FTO	3.573	0.595	0.441	0.939
Pandanus amaryllifolius leaves	TiO_2/ITO	GPE	Pt/ITO	1.610	0.360	0.410	0.240
	TiO_2/FTO	GPE	Pt/FTO	1.190	0.490	0.630	0.390
	TiO_2/FTO	GPE	Pt/FTO	1.910	0.480	0.560	0.510

	Photoanode	Electrolyte	Counter electrode	J_{sc} (mA cm^{-2})	V_{oc} (V)	*FF*	η (%)
Banana leaves (dried)	TiO_2/FTO	I^-/I_3^- LE	Pt/FTO	1.770	0.596	0.492	0.522
Peach leaves (dried)	TiO_2/FTO	I^-/I_3^- LE	Pt/FTO	2.555	0.611	0.422	0.659
Black tea leaves	TiO_2/FTO	I^-/I_3^- LE	Pt/FTO	0.390	0.550	0.400	0.080
Coccinia indica leaves	SnO_2/FTO	I^-/I_3^- LE	Not stated	0.700	0.540	0.610	0.260
	La-SnO_2/FTO	I^-/I_3^- LE	Not stated	0.820	0.540	0.540	0.290
	La-Cu-SnO_2/FTO	I^-/I_3^- LE	Not stated	1.010	0.560	0.510	0.310
Ficus retusa Linn.	Au-TiO_2/ITO	$Ce^{4+/3+}$ LE	Pt/ITO	7.850	0.520	0.289	1.180
Garcinia suubelliptica	Au-TiO_2/ITO	$Ce^{4+/3+}$ LE	Pt/ITO	6.480	0.322	0.331	0.691
Perilla	TiO_2/FTO	I^-/I_3^- LE	Pt/FTO	1.360	0.522	0.696	0.500
Petunia	TiO_2/FTO	I^-/I_3^- LE	Pt/FTO	0.850	0.616	0.605	0.320
Eggplant pulp	TiO_2/FTO	I^-/I_3^- LE	Pt/FTO	0.350	0.630	0.390	0.090
Festuca ovina grass	TiO_2/ITO	I^-/I_3^- LE	C/ITO	1.189	0.548	0.699	0.460
Hierochloe odorata grass	TiO_2/FTO	I^-/I_3^- LE	Pt/FTO	2.199	0.594	0.355	0.460
Torulinium odoratum grass	TiO_2/FTO	I^-/I_3^- LE	Pt/FTO	1.004	0.654	0.483	0.320
Dactyloctenium aegyptium grass	TiO_2/FTO	I^-/I_3^- LE	Pt/FTO	0.698	0.719	0.481	0.240
Moss bryophyte *(hyophila involuta)*	TiO_2/FTO	GPE	Pt/FTO	5.780	0.600	0.570	1.970
	TiO_2/FTO	GPE	Pt/FTO	4.590	0.610	0.640	1.770
	TiO_2/FTO	GPE	Pt/FTO	5.960	0.580	0.580	2.000
	TiO_2/FTO	GPE	Pt/FTO	3.710	0.640	0.720	1.690
	TiO_2/FTO	GPE	Pt/FTO	5.370	0.550	0.730	2.170
	TiO_2/FTO	GPE	Pt/FTO	8.440	0.540	0.580	2.620
Rhoeo spathacea (Sw.) Stearn	Au-TiO_2/ITO	$Ce^{4+/3+}$ LE	Pt/ITO	10.900	0.496	0.274	1.490
Sargassum wightii (marine seaweed)[b]	ZnO/FTO	I^-/I_3^- LE	Pt/FTO	0.203	0.330	0.460	0.070

	Photoanode	Electrolyte	Counter electrode	J_{sc} (mA cm^{-2})	V_{oc} (V)	*FF*	η (%)
Kelp (brown algae)	TiO_2/TCO	I^-/I_3^- LE	Pt/TCO	0.433	0.441	0.620	-
Undaria pinnatifida (brown seaweed)	TiO_2/FTO	I^-/I_3^- LE	Pt/FTO	0.800	0.360	0.690	0.178
	TiO_2/FTO	I^-/I_3^- LE	Pt/FTO	10.700	0.530	0.600	3.400
	TiO_2/FTO	I^-/I_3^- LE	Pt/FTO	13.800	0.570	0.580	4.600
	TiO_2/FTO	I^-/I_3^- LE	Pt/FTO	8.600	0.470	0.600	2.500
	TiO_2/FTO	I^-/I_3^- LE	Pt/FTO	9.000	0.470	0.610	2.600
Cladophora sp. (green algae)	TiO_2/FTO	I^-/I_3^- LE	Pt/FTO	0.145	0.585	0.590	0.055
Green algae (fresh)	TiO_2/FTO	I^-/I_3^- LE	Pt/FTO	0.134	0.416	0.210	0.010
Green algae (dried)	TiO_2/FTO	I^-/I_3^- LE	Pt/FTO	0.397	0.559	0.440	0.100
Chlorella vulgaris (microalgae)	TiO_2/FTO	I^-/I_3^- LE	Pt/FTO	2.530	0.551	0.650	0.900

[a]Intensity 80 mW cm^{-2}.
[b]Intensity 45 mW cm^{-2}.
LE: liquid electrolyte; GPE: gel polymer electrolyte; PEDOT: poly(3,4-ethylenedioxythiophene).

Table 1. The photovoltaic performance of some chlorophyll-sensitized DSSCs.

Carbon structure CE was proposed for quasi-solid-state DSSC using polyethylene oxide (PEO) based gel electrolyte Jeong et al. [27]. Jeong et al. [27] state that activated charcoal-doped MWCNT demonstrate good electrochemical characteristics of high conductivity, excellent electron transport, and facile redox reaction. In addition, this cell was concluded with 10.05 % efficiency showing possibility for large-scale production [27]. Figure 12 illustrates the photovoltaic performance of activated charcoal-doped MWCNT, figure 13 show activated charcoal-doped MWCNT hybrid sandwich structure.

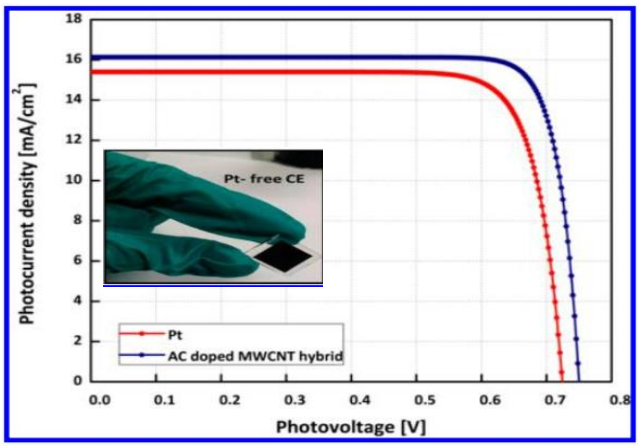

Figure 12 Comparison of photovoltaic performance of quasi-solid-state DSSCs based on PT and AC-doped MWCNT hybrid CE (figure insert shows the proposed AC-doped MWCNT DSSC) [27].

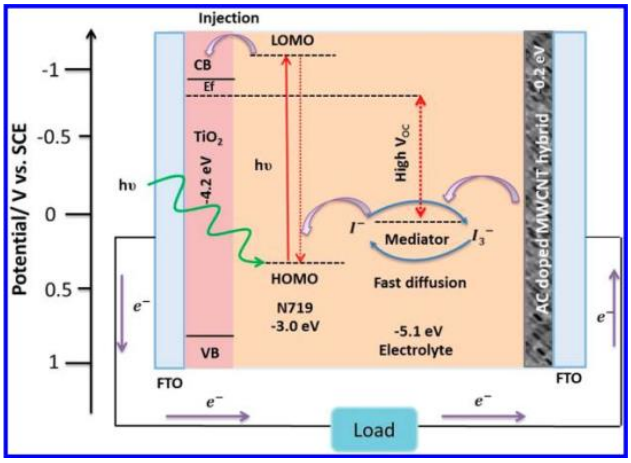

Figure 13 Activated charcoal-doped Multi-Wall Carbon Nano Tube DSSC mechanism, producing electrons that flow through a load [27].

Fill factor of 24.9 %, 365 mV open circuit voltage, and 45 µA short-circuit current was reported for chlorophyll extracted from papaya and jatropha leaves [28]. However, electron collection efficiency of the cell was low and as such the photon conversion efficiency was also low [28].

In another research by Memon et al. [29] highly photocatalytic active and conductive cotton, polyester and linen fabric CE for DSSCs, printed with mesoporous activated charcoal intercalated acid modified carbon nanotubes (M-AC/CNT) were studied (figure 14). For high conductivity, electro-catalytic activity, and electro-catalyst, various concentrations of activated charcoal were added which improved the photocatalytic activity by 52 % [29]. Memon et al. [29] showed 6.26 % photovoltaic conversion efficiency for polyester fabric, 6.06 % cotton and 5.80 % for linen fabrics.

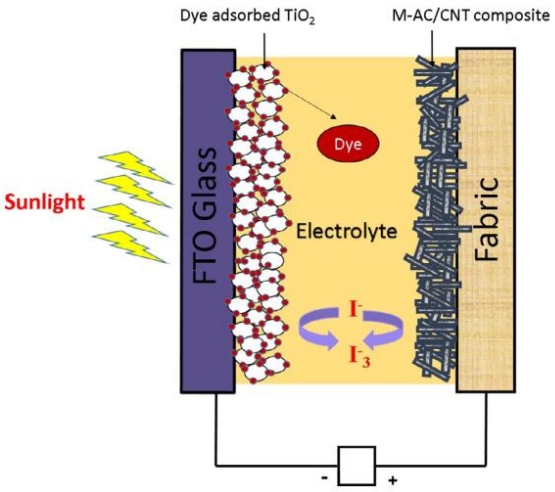

Figure 14 Fabric based DSSCs, display dye adsorbed on titania, electrolyte, activated charcoal composite, and fabric counter electrode [29].

Alhamed et al. [31] conclude that natural dyes demonstrate good photovoltaic performances compared to Ru dye N3 used for Grätzel cells. They reported an efficiency of 3.04 % for their cell [31]. Table 2 shows the findings of this study, however, only information on chlorophyll dye and the combination of dyes were extracted.

Table 2 The open circuit voltage (V_{oc}), short circuit current density J_{sc}, fill factor (FF), and efficiency (η) of the DSSC prepared with chlorophyll (natural) dye [31].

DSSC FTO/TiO_2/Natural Dye/Electrolyte/Pt/FTO	V_{oc} (volts)	J_{sc} (mA/cm^2)	FF %	η %
Chlorophyll	0.225	0.017	54.1	0.04
Combination of dyes	0.420	0.600	60.2	3.04

When a dye has lowest band gap energy, electrons move very fast from the valence band to the conduction band as a result the cell requires small energy for recombination of electrons and this results in high FF [19,29,31].

In the study done by Wang and Kitao [32] efficiency of 2.8 % was reported for DSSCs made from commercially available natural chlorophyll related porphyrin and chlorine sensitizers. Chlorines are believed to have superior light harvesting capabilities than porphyrins thus proper for solar cell applications [32]. Chlorines were made from natural chlorophylls. Table 3 below summarizes the photovoltaic performance of DSSCs made from commercially available natural chlorophyll related porphyrin and chlorine sensitizers.

Table 3 Photovoltaic performance of DSSCs using chlorophyll derivatives [32].

Dye sensitizer	J_{sc} **/mA·cm^{-2})**	V_{oc}**/ V**	**FF**	**%**
Chl-1	2.5	0.47	0.72	0.9
Chl-1-Na	5.7	0.65	0.72	2.7
Chl-2	4.9	0.61	0.69	2.1
Chl-3-Na	1.4	0.50	0.73	0.5

J_{sc}: Short circuit current; V_{oc}: open-circuit voltage; FF: fill factor; η: solar energy-to-electricity conversion efficiency.

1.83 eV was reported for spinach chlorophyll extraction with distilled water, on the other hand, ethanol extraction was 1.88 eV [33]. Adding to that, highest fill factor was obtained for distilled water (0.49 %) and the lowest for ethanol (0.36 %) for the same study [33].

In the search for replacement of Pt CE for DSSC numerous studies were done to study the performance of these materials. Carbonaceous materials were extensively studied.

Metal-free DSSCs were effectively fabricated using an activated carbon filler. This structure showed good electrochemical features with high electronic conductivity [34]. Sun et al. [34] DSSC demonstrated an overall efficiency of 8.48 %. The structural distortion of activated carbon caused high catalytic activity of the cell and in turn can be viewed as a favorable material for effective energy storage [34].

2.4 Status of chlorophyll use as a dye in DSSCs

Chlorophyll by nature converts sunlight to chemical energy in plants for the process of photosynthesis. DSSC converts sunlight into electricity in similar manner as chlorophyll. The structure of a dye must have carboxylic anchoring group which binds strongly to TiO_2, thus ensuring efficient electron injection into the conduction band of TiO_2 [35].

Chlorophyll has available bonds between the dye and TiO_2 molecules via which electrons can move from excited dye molecule to the semiconductor film [36]. However, the performance of chlorophyll is not the same with regards to its structure [35]. Chlorophyll-b displayed good performance compared to its counterpart chlorophyll-a.

Adsorption of chlorophyll onto the photoanode is affected by the state of leaves be it in fresh or dry [37]. Research showed that fresh leaves performed better than dried leaves in terms of efficiency of DSSCs. It is further noted that the period of soaking, pH of the dye and temperature also influence its performance. In addition, 0.290 % efficiency was obtained for chlorophyll extracted from spinach at 60 °C soaking for 12 h [37].

Danladi et al. [38] study displayed an efficiency of 0.040% for chlorophyll pigment extracted from scent leaves. They linked the poor performance of the chlorophyll

pigment to possible absence of anchoring carboxylic groups onto the TiO_2, as well as steric hindrance which blocks the dye molecules from adequately attaching to the semiconductor film.

Due to the possibility of not having anchoring carboxylic groups in chlorophyll, some researches opted for mixing two different dyes. For instance, mixing chlorophyll pigment with anthocyanin pigment. Shah et al. [39] demonstrated the possibility of mixing these pigments, they obtained a conversion efficiency of 0.81% which were extracted from black rice (anthocyanin) and fragrant screw pine (chlorophyll) using methanol as solvent. The better anchoring of anthocyanin to the semiconductor surface and better light absorption by chlorophyll can be attributed to this performance [39].

The poor performance of chlorophyll dye might not be attributed to absence of anchoring bond but rather weak interaction between the anchoring carboxylic group and TiO_2 surface [40]. Furthermore, the extraction solvent could also hamper the performance of chlorophyll dye.

2.5 Analytical methods, spin coating and software

Normally inorganic compound investigation entails the absorption and re-emission of electromagnetic radiation [41]. This provides information on the energy levels of an inorganic compound and the absorption power can be used to give quantitative analytical information [41]. Hence, X-ray and ultraviolet (UV) radiation can be used to determine the electronic states of atoms and molecules, and infrared (IR) radiation can be used to study their vibrational modes. Spin coating, on the other hand, is a method which is used to coat thin films. Once fabrication process is done, the films are assembled as DSSCs and analysed. Sophisticated software, such as edaq Echem are used to plot an IV-curve.

2.5.1 Ultraviolet-visible (UV-vis) spectroscopy

Shriver and Atkins [41] define ultraviolet-visible spectroscopy (UV-vis) as the observation of absorption of electromagnetic radiation in the UV and visible regions of the spectrum (electronic spectroscopy). Roberson et al. [42] classified UV-vis spectroscopy as a qualitative analysis method which can be used for identifying functional groups and structures of molecules that have unsaturated bonds. However, this method does not show molecular weight or tell the presence of saturated bonds in a molecule of interest [42].

Molecular absorption spectroscopy operates on the principles of Beer's law, which incorporates measurement of transmittance (T) or the absorbance (A) of solutions contained in transparent cells on a path length (b, cm) and the concentration of the absorbing material (c). Where ε is the molar absorptivity constant. Beer's law is expressed as [43]: $A = \varepsilon bc$

UV-vis detector has 4 chambers through which the detector analyses molecules, a) light source, b) wavelength selector, c) sample and d) light detector. Harris [44] summarizes the mechanism: the irradiance of the beam decreases when light is absorbed by a sample; light is filtered as single wavelength based on one colour; this light then hits the sample; finally, this absorption is read out by the detector.

2.5.2 Infrared (IR) spectroscopy

Vibrational spectroscopy is used to characterize compounds in terms of the strength, stiffness, and number bonds that are present [41]. In addition, it is also used to detect the presence of known compounds, monitor changes in the concentration of a species during a reaction, determine the components of an unknown compound, determine a likely structure for a compound, and to measure properties of bonds [41]. Also,

infrared spectroscopy can give data on functional groups that are found in the sample [42]. The fingerprint technique makes it a useful qualitative method, and is often used as a quantitative method [42].

Vibrational spectroscopy observations are made on the degrees of vibrational freedom. The movement of molecules with 3n degrees of freedom can be described in terms of translational, vibrational and rotational motions of the molecule [44].

2.5.3 Spin coating

Spin coating is technique used for deposition of a fluid onto a substrate. It uses centrifugal force to evenly coat the substrate forming a thin film on the surface. Spin coating is achieved through dropping of liquid onto substrate surface, followed by a high-speed spin to the substrate to obtain a uniform thin film. Moreover, dynamic and static dispense methods are mostly used in spin coating. Dynamic dispense spin coating method involves the coating of substrate at two different revolutions per second (rpm), 500 rpm and 3000 rpm as in this study. Static spin coating, conversely, is done in one revolution step. In this technique (spin coating), speed of spin coating plays a key role.

2.5.4 Echem (edaq) software

Echem software is used for the collection, display and analysis of data from electroanalytical voltammetric as well as amperometric electrochemical experiments coupled to a potentiostat [45]. Moreover, it uses the e-corder hardware as the digital waveform generator, and data acquisition system [45].

2.6 Degussa Powder (P25)

Degussa P25, TiO_2 powder is a standard material for photocatalytic reactions studies. It contains anatase and rutile [46]. Its electronic structure, light absorption properties, and charge transport features makes it possible to be used in photocatalysis [47]. Due to the large surface area (49 m^2g^{-1}) of P25 powder, P25 powder is used in photocatalytic reactions. The transfer of photoexcited electrons and positive holes between anatase and rutile particle connection is believed to boost the charge separation and thus enhance the efficiency of electron-hole pair usage [48]. Transmission electron microscopic (TEM) images and diffuse reflectance spectra of Degussa showed transformation of anatase surface crystals to that of rutile structure as cited by Thiruvenkatachari [47] from Bickley et al. [48] works. In another study, again as cited by Thiruvenkatachari [47] TEM analysis showed single crystalline structures separately for anatase and rutile in Degussa.

Commercially available anatase has size <50 nm with 3.2 eV band gap energy, this corresponds to 385 nm wavelength [49]. Rutile, on the other hand, has >200 nm size with 3.0 eV which relates to 410 nm wavelength [46]. Like any other semiconductors, the P25 powder operates on the principle mechanism of a semiconductor for photocatalytic reactions. Upon charging of light with the same amount of energy or larger than that of the E_g, electrons are promoted from the valence band to the conduction band. Positive holes are created in the valence band and electrons in the conduction band.

TiO_2 does not absorb visible light. As a result, TiO_2 is doped with a dye which absorbs visible light for photoactivation [49]. It is believed that TiO_2 uses only 5 % of the incident solar irradiation for photocatalytic reaction, thus limiting its everyday use.

CHAPTER 3: RESEARCH METHODS

3.1 Research Design

Figure 15 illustrates the research design for this study. Precursor solution was used to fabricate (create) titania precursor solution (**$S_{titania}$**) thin film, which was used as a block layer for the titania paste and the CARBO-chac counter electrode (CE). The thin film with the titania paste was immersed in chlorophyll dye extracted from a local plant leaf (mopane leaves), using methanol as the solvent extraction, and assembled in the DSSC.

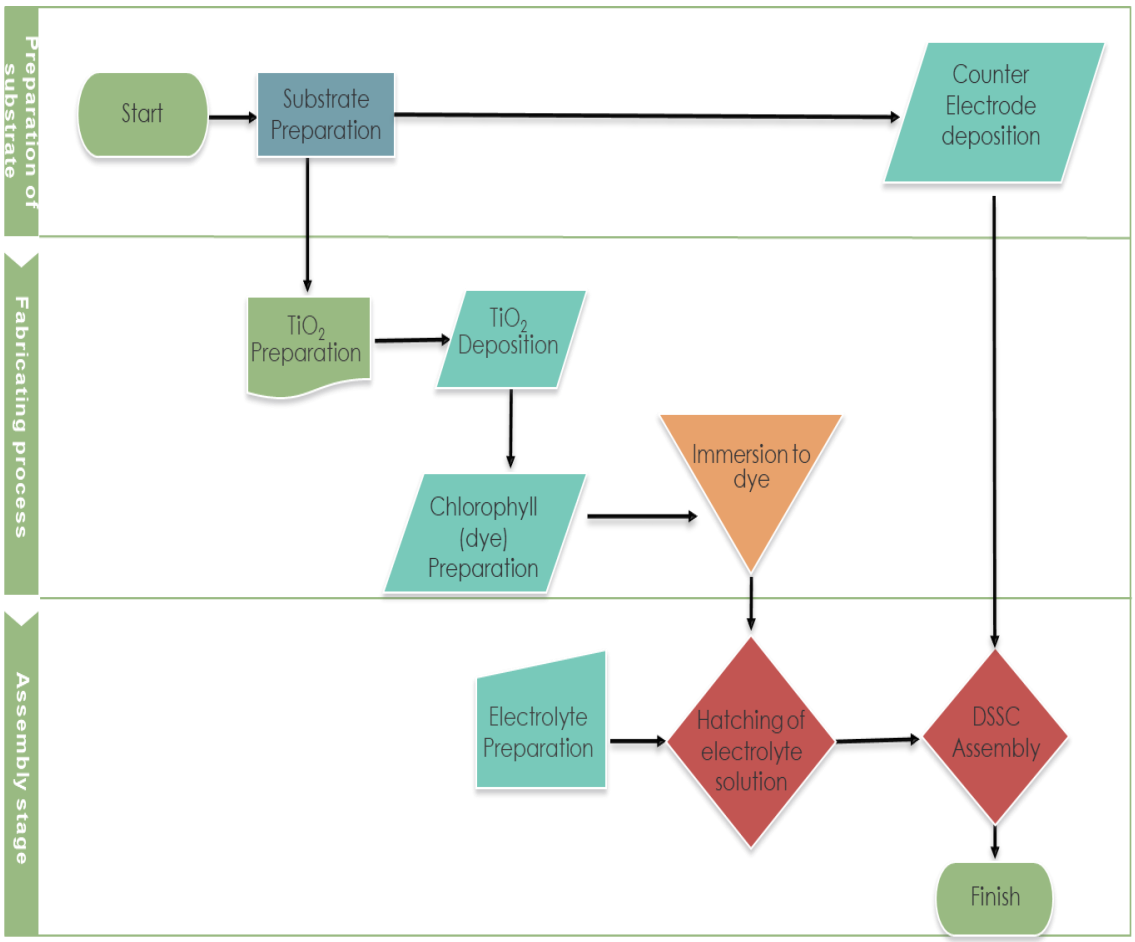

Figure 15 Scheme for the assembled DSSC research design.

3.2 Procedures

3.2.1 Cleaning of FTO glass substrate and determination of the conductive side of FTO glass substrate after cleaning

The FTO glass substrates were soaked in ethanol for 2 minutes, and washed with acetone. The glass substrates were then rinsed with deionized water. Thereafter, it was dried in air for 10 minutes.

After cleaning FTO glass substrate, the conductive side of the glass substrate was determined using a multimeter. The meter was set to measure Ohms and both leads were put on one side of the slide, resistance measured was near zero, that was the conductive side.

The spin coating of precursor solution, the spreading of titania paste, and spreading of CARBO-chac paste onto the FTO glass substrate, must be done on the conductive side of the FTO glass substrate. That is the reason for the determination of conductive side of the FTO glass substrate after cleaning.

3.2.2 Preparation of Titania precursor ($S_{titania}$) solution and spin coating of $S_{titania}$ onto FTO glass substrate.

Molecular Precursor Method (MPM) [17] was used to prepare the $\mathbf{S_{titania}}$ solution. 10.00g Ethanol was added to 10.00g Methanol. To the mixture, 3.65g ethylenediaminetetraacetic acid (EDTA), followed by 3.55g dibutylamine was added. After refluxing for 2 hours, the solution was cooled to room temperature. After the solution cooled to room temperature, 3.55g titanium tetraisopropoxide was added to the solution and refluxed for 4 hours and 30 minutes. The solution was then cooled to room temperature, to this solution, after it has cooled to room temperature, 1.56g hydrogen peroxide was added and again the solution was refluxed for half an hour (i.e.

30 minutes). After 30 minutes the solution was cooled to room temperature. Scheme 1 below outlines the procedures for preparing $\mathbf{S_{titania}}$ solution.

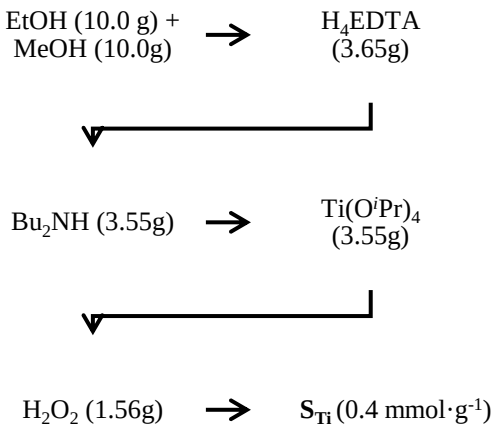

Scheme 1 Preparation of $\mathbf{S_{titania}}$ solution.

After successful preparation of $\mathbf{S_{titania}}$ solution, it was then used to prepare the $\mathbf{S_{titania}}$ thin film. The FTO glass substrate was cleaned and the conductive side determined as outlined under section 3.2.1. Thereafter, the precursor solution, was spin coated on the conductive side of the FTO glass substrate as indicated in scheme 2. Spin coating is method of fabricating thin films which is used to deposit ultra-thin films on substrates. This is done by allowing enough precursor solution to spread evenly on the glass substrate. Next, this thin film was heated at 600 °C for 30 min. Heat treatment was done to eliminate any organic ligands from the resultant precursor thin film. The resultant thin film was preserved for the use as a blocking layer.

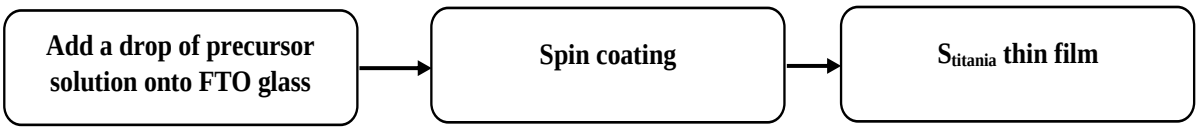

Scheme 2 Spin coating $\mathbf{S_{titania}}$ solution on FTO glass substrate.

3.2.3 Doctor blade method

Doctor blade method is a coating technique, applied to coat the TCO glass, with paste, for photo anode and counter electrode. In this study coating was done by this method (figure 16). Before coating, the FTO glass substrate was tape casted on the lab bench, maintaining an area of 78.3 mm^2. The paste waste kept at an edge of the FTO glass substrate for filling. For uniform coating, the glass rod was swept in a rapid motion towards the bottom of the FTO glass substrate, and then again in the reverse direction. Without lifting the glass rod same movement was applied 2-3 times. After coating the paste, tapes were removed carefully, without ruining the paste layer.

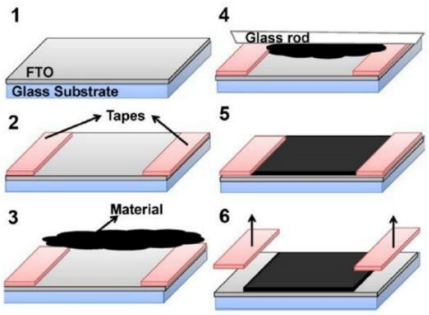

Figure 16 Step by step Doctor blade method for coating TCO glass substrate using paste, adapted from Raihana's study [50].

3.2.4 Preparation of CARBO-chac paste

Raihana's [50] method was used to prepare graphene paste. 5.00g CARBO-chac was placed in a beaker. Ethanol, ethylene glycol and water were added dropwise to CARBO-chac until a smooth paste was obtained.

3.2.5 Fabricating TiO_2-CARBO-chac structure

FTO glass substrate was cleaned and the conductive side determined as outlined under section 3.2.1. On the fabricated $\mathbf{S_{titania}}$ thin film (used as a blocking layer), CARBO-

chac paste was coated using Doctor blade method (section 3.2.3). Thereafter, CARBO-chac paste FTO glass substrate was heat treated at 50 °C for 5 minutes.

3.2.6 Preparation of Titania paste

Raihana's [50] method was used to prepare Titania paste. 2.50g Degussa powder was placed in a beaker, and few drops of acetic acid was added dropwise until a smooth paste was obtained.

3.2.7 Preparation of Chlorophyll dye

The Chlorophyll was extracted from the *Colophospermum Mopane* leaves (Mopane leaves) to prepare Chrolophyll dye as outlined by Kalipi [51] in her research. Dry Mopane leaves were obtained from Northern Namibia (Omusati Region). These leaves were crushed to a fine powder, 20g of powdered dry leaves were placed in a beaker, and 200ml Methanol was then added. The mixture was filtered and stored for analysis, and use in fabricating TiO_2-Chlorophyll film.

3.2.8 Fabricating TiO_2-Chlorophyll sandwich structure

FTO glass substrate was cleaned and the conductive side determined as outlined under section 3.2.1. On the conductive side of the glass substrate (fixed with scotch tape), adopting doctor blade method (section 3.2.3), titania paste was coated on the surface of the $\mathbf{S_{titania}}$ FTO glass substrate (conductive side). The glass with the paste was then dried in air, at room temperature, over 4 hours and then heated at about 420 °C, to remove any inorganic residue, for another 20 minutes. After 20 minutes elapsed, it was cooled to room temperature. The glass with the titania paste was put in a petri dish.

Next, chlorophyll dye was then added dropwise (slowly) onto the surface of the paste using a pipette until it was completely covered with the dye. After 20 minutes, the

glass substrate was removed from the petri dish, and the sides of the glass with no paste were rinsed with ethanol to remove any residual dye on the glass substrate.

3.2.9 Preparation of the Iodide electrolyte

The triiodide electrolyte was prepared by using Raihana's [50] method. Iodide crystals (0.254 g) were dissolved in 20 ml ethylene glycol (EG). Potassium iodide (0.8213 g) was added and the solution was then stirred till it dissolved. This solution was then stored as KI/I_2 electrolyte solution in a brown stock bottle for use at a later stage. The KI/I_2 electrolyte solution is sensitive to light and thus need to be stored in a container where it does not react with light, in this case the brown stock bottle was used.

3.2.10 Assembling TiO_2-CARBO-chac-TiO_2-Chlorophyll sandwich based DSSC

The two fabricated (constructed) films, TiO_2-CARBO-chac structure and TiO_2-Chlorophyll structure, were assembled together in a sandwich form. TiO_2-CARBO-chac structure was placed on top of the TiO_2-Chlorophyll structure. Plastic was used to seal the assembled sandwich based DSSC with a clear adhesive. A small hole was left in the plastic sealing for injection of electrolyte solution. After the complete assembly of the cell, it was then inspected for any defects. After inspection, few drops of KI/I_2 electrolyte solution was injected into the cell. Finally, the photo-voltage of the assembled TiO_2-CARBO-chac-TiO_2-Chlorophyll sandwich based DSSC was measured.

Since measurements were taken outdoor, solar radiation that is received by Namibia was used, which is ~5.8 – 6.4 kWh/m^2, assembled solar cell was exposed to sun for 30 minutes.

Following test conditions were applied: ~0.58 mW/cm^2 solar radiation, 7.83 cm^2 cell area, 1 sun = 1.5 AM air mass, ~30 °C surrounding temperature, 0 m/s wind speed (no

wind blew), with clear sky. The assembled cell was place at 45° angle facing the sun when measurements were taken.

CHAPTER 4: RESULTS AND DISCUSSION

4.1 The fabricated $S_{titania}$ thin film

Transparent **$S_{titania}$** thin film was obtained after it was annealed at 600 °C, remove any organic ligands for 30 min. This thin film was later used as photoanode (blocking

layer), and counter electrode (also blocking layer). Figure 17 b below shows the fabricated **S**$_{titania}$ thin film.

a) b)

Figure 17 a) Titania precursor solution (**S**$_{titania}$), and b) fabricated **S**$_{titania}$ thin film.

4.2. The absorption spectrum of the fabricated TiO_2 on FTO

TiO_2 prepared by MPM on FTO conductive glass substrate absorb visible light, so that photo absorptions from solar energy may became more effective and can achieve higher efficiency. In figure 18, the peak at 400 nm wavelength shows the absorption of visible light by titania on FTO glass substrate.

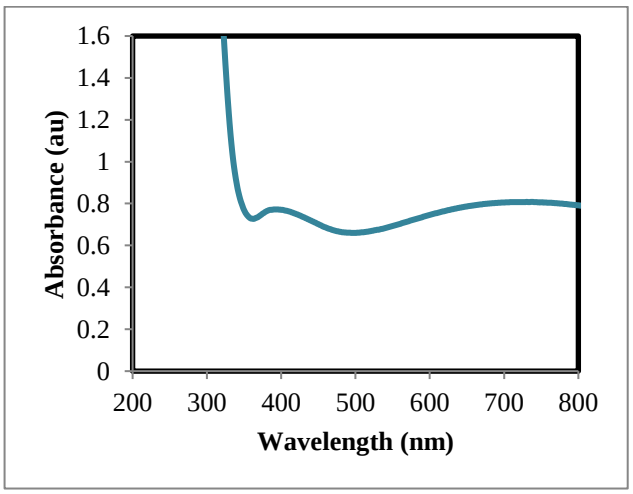

Figure 18 Absorption spectrum of TiO_2 on FTO conductive substrate (glass), which shows an adsorption peak at 400 nm wavelength, adapted from Daniel [18].

4.3 Titanium dioxide (P25, Degussa) paste fabricated thin film

The fabricated $\mathbf{S_{titania}}$ thin film was later used to prepare the titanium dioxide thin film which was constructed using Degussa paste (figure 19). Using doctor-blade method, Degussa paste was deposited onto the fabricated $\mathbf{S_{titania}}$ thin film. Next, the substrate was dried in air for 4 hours. When the layer is too thin, cracks would form thus the paste should be slightly thick. However, cracks also sometimes show complete drying of a substance. This can be attested by figure 19 as the paste was completely dried after the 4 hours elapsed. Again, heat treatment was done, this time, to successfully deposit the paste onto the precursor thin film after the 4 hours of air drying. A white paste was obtained after the heat treatment. Thickness of this paste layer can be referenced to the scotch tape that was fixed on the glass substrate when coating was done. This titanium dioxide paste film was used as a photoanode in the assembly of the DSSC.

Figure 19 Fabricated Titanium dioxide paste FTO glass substrate after air drying.

4.4 Fabricated CARBO-chac paste thin film

The fabricated CARBO-chac paste layer thickness can also be referenced to the thickness of the scotch tape that was fixed on the FTO glass substrate when CARBO-chac paste coating was done. After successful mass deposition, the paste bonded to the surface of the FTO glass substrate, by heat treatment, CARBO-chac paste FTO glass substrate (figure 20) was used as the CE in the DSSC assembly.

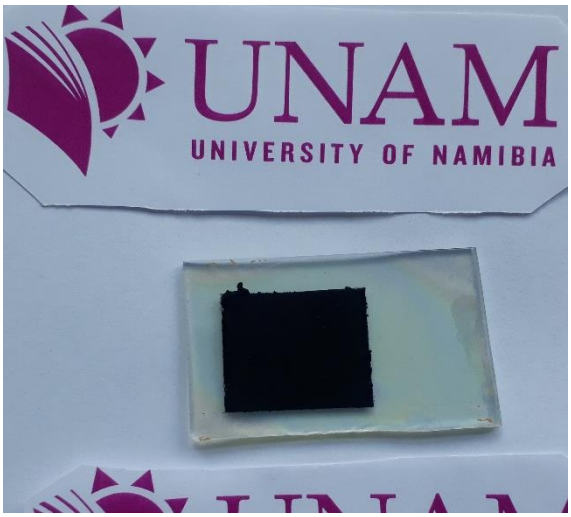

Figure 20 Fabricated CARBO-chac paste FTO glass substrate (done at 50 °C heat treatment).

4.5 Chlorophyll dye extracted from *Colophospermum Mopane* leaves

Chlorophyll dye was successfully extracted from *Colophospermum Mopane* (mopane) leaves. The solvent of extraction that demonstrated good extraction of chlorophyll was methanol. Other solvents showed poor extraction of the chlorophyll from the mopane leaves. Chlorophyll is pigment that absorb green wavelength hence its green color. The extracted chlorophyll via methanol solvent displayed a dark green color compared to ethanol (pale green) and hexane (no color change). Figure 21 b shows the extracted chlorophyll dye via methanol solvent.

a)

b)

Figure 21 a) Mopane plant leaves b) Chlorophyll dye extracted in methanol solvent from the mopane plant leaves.

4.6 Infrared and absorption spectrum for the extracted Chlorophyll dye

4.6.1 Infrared spectrum of the extracted Chlorophyll dye

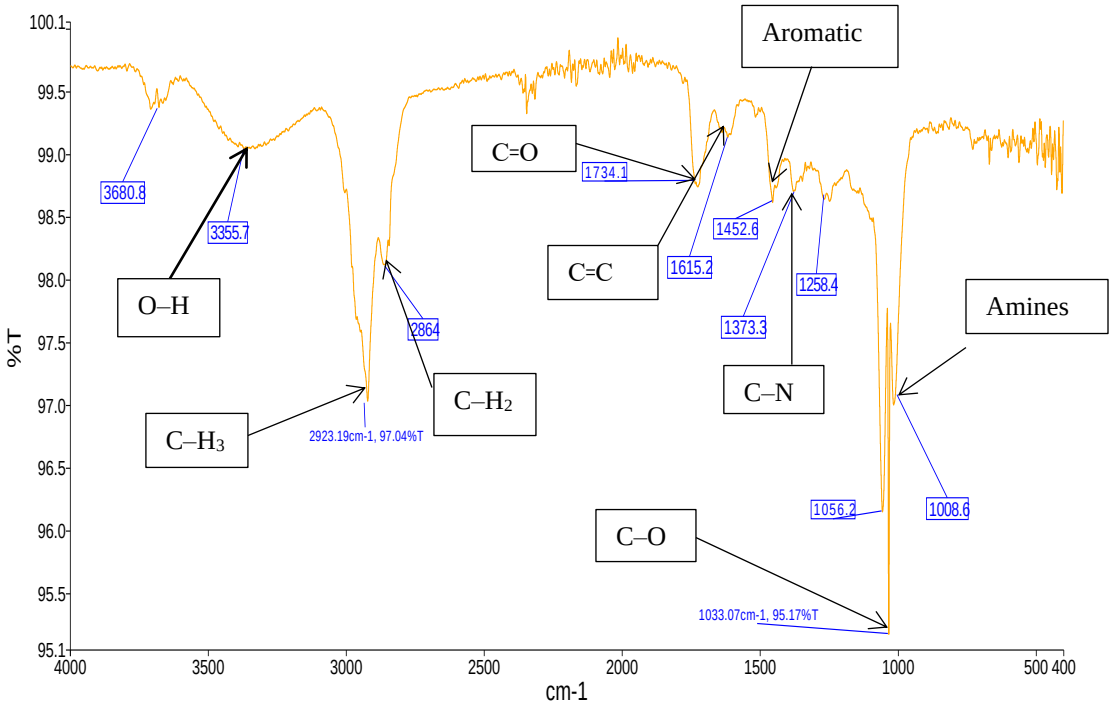

Figure 22 Infrared spectrum of the Chlorophyll dye extracted from Mopane dye, adapted from Kalipi's study [51].

The OH stretch can be observed at 3356 cm^{-1}, carbonyl stretch at 1734 cm^{-1}, the aromatic stretch at 1453 cm^{-1}, methyl (CH_3) and CH_2 stretch at 2923 cm^{-1}, and 2864 cm^{-1} respectively. In addition, amine stretch can also be observed at 1009 cm^{-1}, CN stretch at 1373 cm^{-1}. A band in the double bond region, at 1615 cm^{-1}, as a result of C=C vibrations can be observed. These observations are correlating to the structure of chlorophyll and comparable with the data from available literature, thus can be conferred that the extracted dye is indeed chlorophyll.

4.6.2 Absorption spectrum of the extracted Chlorophyll dye

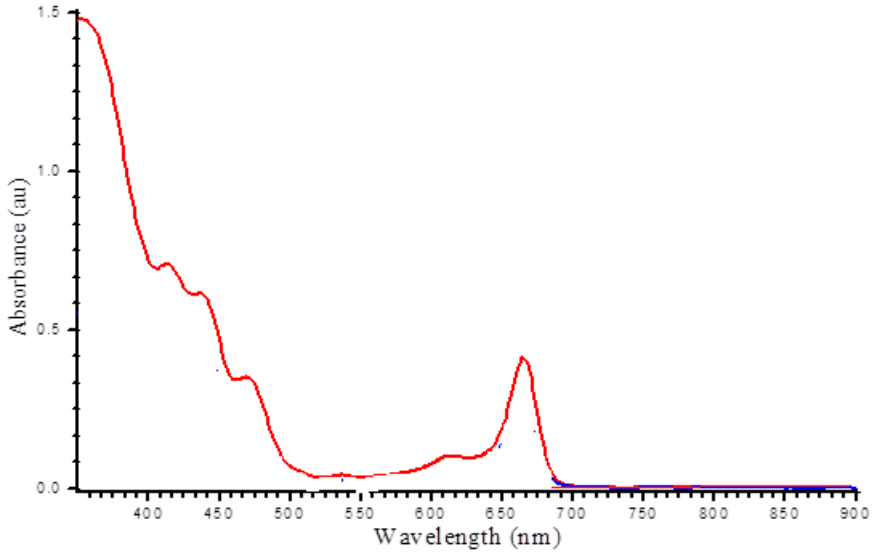

Figure 23 UV-vis absorption spectrum of Chlorophyll dye sensitizers, adapted from Kalipi's research [51].

Two prominent absorption peaks can be noted at the 480 nm and 675 nm wavelengths. From literature, chlorophyll absorb visible light in the range of 420 nm and 600 nm wavelength [8-10, 14]. Data obtained is consistent with literature. Hence, the data confirms that the chlorophyll extracted from mopane leaves is indeed chlorophyll and does absorb visible light.

4.7 Preparation of the Photoanode

The fabricated titanium dioxide paste layer (figure 19) was later soaked chlorophyll dye extract for 20 minutes. Making the soaking process for longer period of time can give dye molecules ample time to adequately attach or bind to the surface of the nanoporous titanium dioxide layer (figure 24). This nanoporous layer is simply used as a binding side for the extracted chlorophyll dye molecule. Instead of dropping the thin films face down, the dye was added dropwise onto the nanoporous titanium dioxide. This method allows sufficient adsorption of dye molecules onto the nanoporous titanium dioxide surface compared to the conventional face down dip.

Figure 24 shows titanium dioxide thin films soaked in the chlorophyll dye. The green striking color can be clearly seen in figure 24, thus we can conclude that the dye extract is indeed chlorophyll.

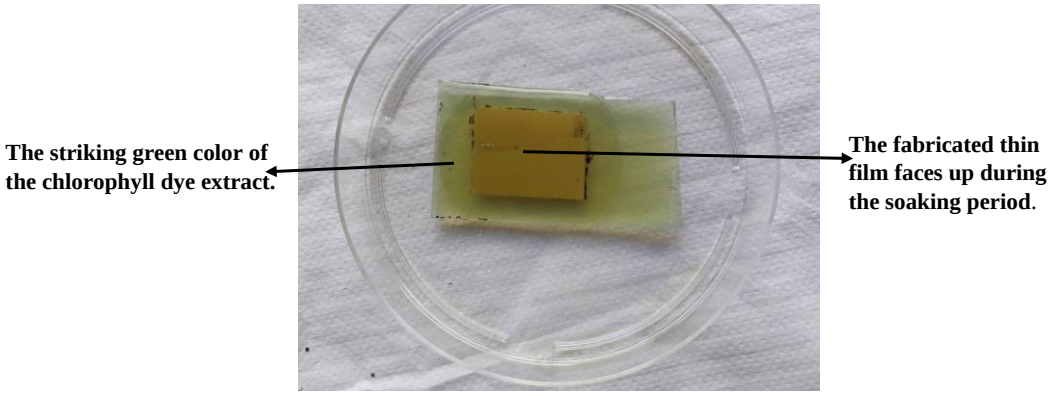

Figure 24 Titanium dioxide thin film soaked in chlorophyll dye extract (face up).

After the soaking period was over, the white nanoporous titanium dioxide thin film displayed a green color (figure 25). This change in color is due to the adsorption of the chlorophyll dye molecules on its surface. The resultant thin film was used as the photoanode for the cell.

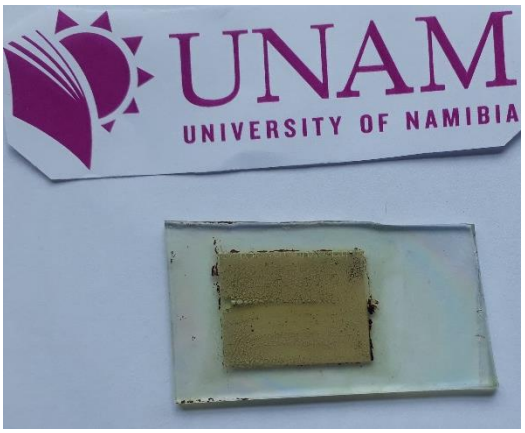

Figure 25 Chlorophyll dye sensitized titanium dioxide thin film.

4.8 Assembly of the DSSC

After all the components of the DSSC were ready, the cell was assembled together. The active side of the fabricated photoanode and fabricated counter electrode were facing each other. Meaning, the fabricated titanium dioxide thin film and CARBO-chac fabricated thin films face each other. A space was left to accommodate the electrolyte. The DSSC design was $2.7 \times 2.9\ cm^2$ (figure 26).

Electrodes can be squeezed together, and the electrolyte introduce into the cell via capillary effect. On the other hand, the electrodes can be wrapped and electrolyte injected into the cell via the holes made through the cathode.

The squeezing method is formally known as the open cell because the internal area of the solar cell is uncovered or rather in air. Nevertheless, the electrolyte would not be kept in the cell and later the cell will dry. This method only applies to practical applications and as a result of sealing method it faces a stability problem.

The second method contrary to the first approach is the best choice as it is highly stable. The electrodes are joined together with a spacer so that the electrolyte is confined in the void. Though this is time consuming, it enables the DSSC to work for longer period of time.

Since this study is research based, and would like to have results which could benefit the research community, the second approach seemed to fit this study. In other words, the second method (spacing) was used to assemble the DSSC.

In the space between the two electrodes, the electrolyte was injected into the DSSC via the hole that was left in the sealant. Once assembled the cell was put to test.

A multimeter was connected, negative terminal to the photoanode (titania electrode) and positive terminal the counter electrode. The open circuit voltage and short circuit current of the solar cell were measured under full sun illumination.

Smaller notch of microamps and millivolts were observed. The resistance of the cell was also found to be low. The current and voltage values for the cell were 170.8 µA and 510 mV respectively. The resistance, on the other hand for the assembled DSSC was 0.931 Ω. When the cell was covered with A4 hard cover notebook (an opaque object), no sunlight or rather sunrays reached the cell, the values dropped significantly. This means that the cell possibly performs best under direct sunlight.

After a week of assembly, photovoltaic measurements were again taken in order to determine the stability of the dye as well the electrolyte. It was found that similar readings were obtained for the cell.

The assembled cell was also tested with a solar motor. However, this cell did not power the motor possibly due to its size and exposed surface area which is 7.83 cm^2, considered very small.

a) b)

Figure 26 a) side view, b) and top view of the assembled Dye Sensitized Solar Cell using FTO-TiO_2-CARBO-chac-Chlorophyll-TiO_2-FTO Sandwich Structure.

4.9 The photovoltaic performance (photo-electrical conversion efficiency) of the assembled cell

The photovoltaic performance of this assembled DSSC was measured using a multi-meter under direct sunlight illumination. An external current flow when sunlight shine on the anode side of the cell. For complete darkness, the cell was placed in sealed back. This was to test whether the cell can operate under no light.

Furthermore, the assembled cell was then connected to the Potentiostat 466. The machine automatically plots the IV-curve, figure 27, for the assembled cell using Echem software.

Test conditions: ~0.58 mW/cm^2 solar radiation, 7.83 cm^2 cell area, 1 sun = 1.5 AM air mass, ~30 °C surrounding temperature, 0 m/s wind speed (no wind blew), with clear sky. The assembled cell was place at 45° angle facing the sun when measurements were taken.

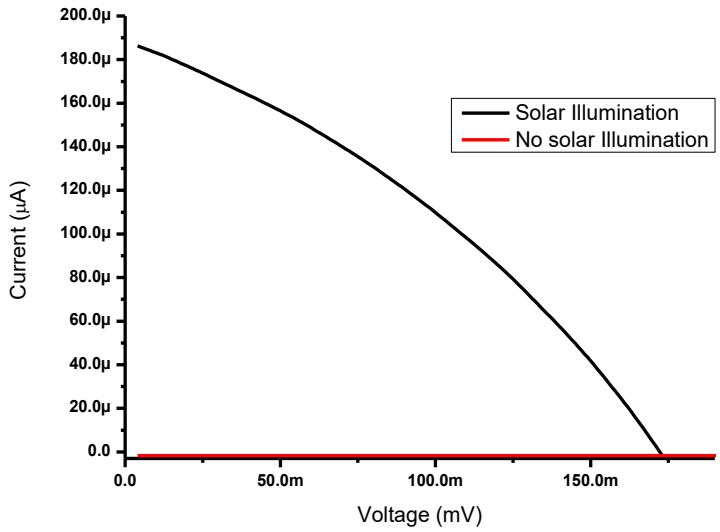

Figure 27 IV curve for the assembled Dye Sensitized Solar Cell, TiO_2-CARBO-chac-Chlorophyll-TiO_2 Sandwich Structure.

It can be noted from the IV-curve, figure 27, that the best operation of the cell is under illumination (light). Under no illumination, the IV-curve shows a zero potential. This implies that the cell does not produce power when it is completely dark (no light).

Fill factor was obtained by dividing area A with area B (figure 28), the efficiency of the assembled cell was obtained as follows:

$$FF = \frac{I_{mp}V_{mp}}{I_{sc}V_{oc}} = \frac{Area\ A}{Area\ B} = \frac{109\ mV\ \times 100.0\ \mu A}{174\ mV \times 187.0\ \mu A} = 0.335 = 33.5\ \%$$

$$\eta = \frac{FF \times I_{sc} \times V_{oc}}{P_{solar}} \times 100\% = \frac{0.335 \times 170.8\ \mu A \times 287.1\ mV}{4.5\ mW} \times 100\ \% = 0.37\ \%$$

$\mathbf{P_{solar}}$ was obtained by multiplying the solar radiation with the area of the assembled DSSC.

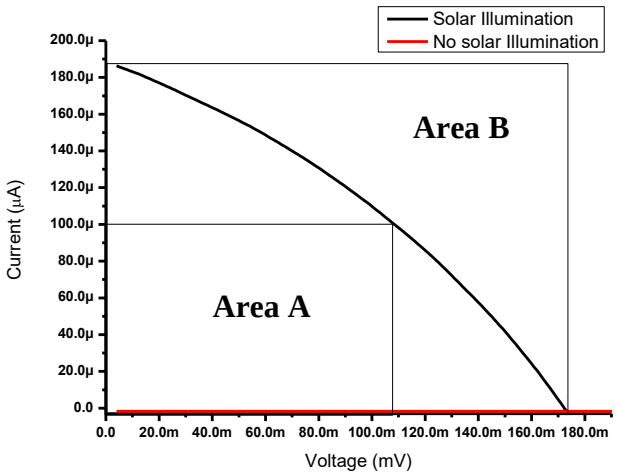

Figure 28 IV curve for the assembled DSSC, used for fill factor calculation.

Table 4 The photovoltaic parameters of the assembled DSSC.

Assembled DSSC	V_{oc} (mV)	I_{sc} (µA)	J_{sc} (mA/cm^2)	FF	η %
Chlorophyll-Charcoal	**287.1**	**170.8**	**0.022**	**0.335**	**0.37**

V_{oc}: open-circuit voltage; I_{sc}: Short circuit current; J_{sc}: Short circuit current density; FF: fill factor; η: solar energy-to-electricity conversion efficiency.

The assembled Chlorophyll-CARBO-chac DSSC efficiency obtained is consistent with the study done by Alhamed et al. [31], which obtained an efficiency of 0.04 %,

and another study done by Danladi et al. [38], which also reported an efficiency 0.04 % for chlorophyll dye, using a Pt counter electrode instead. Moreover, the efficiency obtained for the current study, Chlorophyll-CARBO-chac DSSC, is slightly greater than the efficiency (0.29 %) reported for chlorophyll dye by Arof and Ping [37]. However, the efficiency for the current study is less than the efficiency obtained for the study done by Jeong et al. [27], which was 10.05 %.

4.10 The new model (TiO_2-CARBO-chac-Chlorophyll-TiO_2 Sandwich Structure)

4.10.1 FTO-Titania coupling

Mesoporous photoanode cannot uniformly cover the surface of the entire Fluorine-doped tin oxide (FTO) glass thus in DSSCs the electrolyte makes contact with the FTO glass. Further, at this point which is the FTO-electrolyte boundary, charge recombination limits electron collection and in turn affects photo conversion efficiency (PCE). Alteration of this boundary enhances the performance of DSSCs by overturning the recombination of electrons from the FTO to the electrolyte. This can be achieved by adding compact metal oxide blocking layer onto FTO that would limit the back-electron transport from the FTO to the electrolyte. For the purpose of this study Titania was spin coated onto the FTO glass which was used as a blocking layer for both CE and photoanode. Figure 29 show the assembled DSSC for the current study.

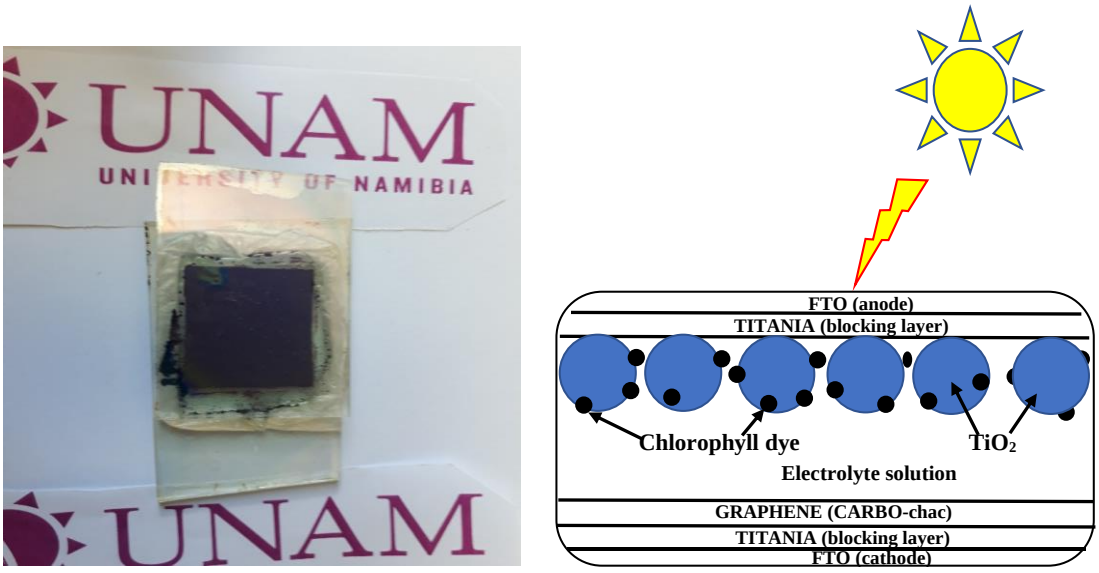

a) **b)**

Figure 29 a) top view, b) and schematic diagram of the assembled Dye Sensitized Solar Cell using TiO_2-CARBO-chac-Chlorophyll-TiO_2 Sandwich Structure.

4.10.2 The mechanism of photo-electric conversion of the chlorophyll-sensitized DSSC

Upon illumination on the cell, the molecules of the chlorophyll Dye (*D*) will be excited (D^*) after absorbing photon (*hv*) [eq 1].

$$hv + D \rightarrow D^* \qquad \text{eq 1}$$

The excited chlorophyll molecules (D^*) will inject electrons into the TiO_2 semiconductor conduction band and the excited dye will then be oxidized or ionized (D^+) [eq 2].

$$D^* + TiO_2 \rightarrow D^+ + e^-_{cb}\,(TiO_2) \qquad \text{eq 2}$$

The oxidized chlorophyll dye molecules (D^+) will accept electrons from an iodide ion (I^-) in the electrolyte when the I- ions are released to the oxidized molecules and in turn oxidized to triiodide ions (I_3^-) [eq 3].

$$2D + 3I^- \rightarrow I_3^- + 2D \qquad \text{eq 3}$$

The electron in the TiO_2 conduction band flows out of the device through the load to reach the counter electrode and reduce the triiodide ion [eq 4].

$$I_3^- + 2e^- \rightarrow 3I^- \qquad \text{eq 4}$$

The iodide ion will be restored, the electron circuit will be completed, and the whole system is back to its original state to start a new cycle. These processes will continue as long as the cell receives light and a resulting current will be produced in the external circuit continuously. When light shines on the cell, the voltage observed is given by the energy difference between the photoanode's Fermi level and the electrolyte's redox potential.

CHAPTER 5: CONCLUSION

In this study thin films were fabricated (constructed) using Molecular Precursor Method (MPM) to assemble the Dye Sensitized Solar Cells using TiO_2-CARBO-chac-Chlorophyll-TiO_2 Sandwich Structure. Chlorophyll dye was successfully extracted from the *Colophospermum Mopane* (mopane) leaves, which was confirmed by the infrared spectrum and UV-vis absorption spectra.

An external flow of current occurred when light shine on the anode. The photovoltaic performance of this assembled DSSC was then measured using a multi-meter under direct sunlight illumination. Furthermore, the assembled cell efficiency was determined by plotting an IV-curve. The current and voltage values for the cell were 157.4 µA and 510 mV respectively. Open circuit voltage, 287.1 mV; short circuit current 170.8 µA; fill factor 0.335 with an efficiency of 0.37 % was obtained.

This study brings hope to those local towns where the *Colophospermum Mopane* plants grow. The leaves normally scatter all over the town causes littering in that specific area. Instead, the leaves could be collected for chlorophyll harvesting. This could help ease the problem of littering in that specific town area. In addition, this could also mean planting more *Colophospermum Mopane* trees at an assembly plant or station where this cell could be fabricated and assembled. Meanwhile, another possibility of reducing global warming. Not only does this study bring hope to local towns but also to the entire Namibian nation as well.

Based on the results that were obtained, the coupling of CARBO-chac can enhance the photocatalytic and photoluminescence properties of titania. In addition, there is a great potential in incorporating activated charcoal (graphene) for the use of counter electrode for Dye Sensitized Solar Cells.

Recommendations:

In the future, the shape and morphology of the cell should be studied. The internal structure cell should also be measured with appropriate instruments, to check the thickness and 3D structure of the assembled cell. Squeezing method of assembly can also be done to check whether the cell can still produce good results.

REFERENCES

1. Kroposki B, Margolis R, Ton D. Harnessing the sun. *IEEE Power and Energy Magazine*. 2009;7(3): 22-33.
2. Fleming RJ. The Source of the Earth's Thermal Blanket and Energy Balance. In: The Rise and Fall of the Carbon Dioxide Theory of Climate Change 2020 (pp. 61-67). *Springer, Cham*.
3. Grätzel M. Dye-sensitized solar cells. *Journal of photochemistry and photobiology C: Photochemistry Reviews*. 2003;4(2): 145-153.
4. McConnell I, Li G, Brudvig GW. Energy conversion in natural and artificial photosynthesis. *Chemistry & biology*. 2010;17(5): 434-447.
5. Lamba R, Shirage PM. *Fabrication of TiO_2 based dye-sensitized solar cell with natural dyes* (Doctoral dissertation, Discipline of Physics, IIT Indore).
6. Matos A, Mendes F, Valente A, Morais T, Tomaz AI, Zinck P, Garcia MH, Bicho MB, Marques F. Ruthenium-based anticancer compounds: insights into their cellular targeting and mechanism of action. *Ruthenium Complexes*. 2018: 164.
7. Tributsch H. Reaction of excited chlorophyll molecules at electrodes and in photosynthesis. *Photochemistry and Photobiology*. 1972;16(4): 261-269.
8. Taya SA, El-Agez TM, El-Ghamri HS, Abdel-Latif MS. Dye-sensitized solar cells using fresh and dried natural dyes. *International Journal of Materials Science and Applications*. 2013;2(2): 37-42.
9. El-Agez TM, El Tayyan AA, Al-Kahlout A, Taya SA, Abdel-Latif MS. Dye-sensitized solar cells based on ZnO films and natural dyes. *International Journal of Materials and Chemistry*. 2012;2(3): 105-110.

10. Abdel-Latif MS, El-Agez TM, Taya SA, Batniji AY, El-Ghamri HS. Plant seeds-based dye-sensitized solar cells. *Materials Sciences and Applications*. 2013;4(09): 516.
11. Wongcharee K, Meeyoo V, Chavadej S. Dye-sensitized solar cell using natural dyes extracted from rosella and blue pea flowers. *Solar Energy Materials and Solar Cells*. 2007;91(7): 566-571.
12. Roy MS, Balraju P, Kumar M, Sharma GD. Dye-sensitized solar cell based on Rose28 Bengal dye and nanocrystalline TiO_2. *Solar Energy Materials and Solar Cells*. 2008;92(8): 909-913.
13. Wang ZS, Cui Y, Hara K, Dan-oh Y, Kasada C, Shinpo A. A high-light-harvesting-efficiency coumarin dye for stable dye-sensitized solar cells. *Advanced Materials*. 2007;19(8): 1138-1141.
14. Etula J. Comparison of three Finnish berries as sensitizers in a dye-sensitized solar cell. *European Journal For Young Scientists And Engineers*. 2012;1: 5-23.
15. Ahmadian R. Estimating the impact of dye concentration on the photoelectrochemical performance of anthocyanin-sensitized solar cells: a power law model. *Journal of photonics for energy*. 2011;1(1): 011123.
16. Hernandez-Martinez AR, Estevez M, Vargas S, Quintanilla F, Rodríguez R. Natural pigment-based dye-sensitized solar cells. *Journal of applied research and technology*. 2012;10(1): 38-47.
17. Nagai H, Sato M. Heat treatment in molecular precursor method for fabricating metal oxide thin films. Heat Treatment—Conventional and Novel Applications; Czerwinski, F., Ed. 2012: 297-322.

18. Daniel LS. Electrical conductivities, Plasmonic properties and vis-responsive activities of Ag-Nanoparticles/ Titania composite thin films fabricated using Molecular Precursor Method (MPM). Dissertation 2014. Kogakuin University, Japan.
19. Sharma K, Sharma V, Sharma SS. Dye-sensitized solar cells: Fundamentals and Current Status. *Nanoscale research letters*. 2018;13(1): 381. Available from: https://doi.org/10.1186/s11671-018-2760-6.
20. University of California, Los Angeles. Extraction of Chlorophyll from Fresh Spinach and Investigation of the Photochemistry of Chlorophyll.
21. Shalini S, Balasundaraprabhu R, Kumar TS, Prabavathy N, Senthilarasu S, Prasanna S. Status and outlook of sensitizers/dyes used in dye sensitized solar cells (DSSC): a review. *Int. J. Energy Res*. 2016;40(10):1303-1320. Available from: doi: 10.1002/er.3538.
22. Martineau D. Dye Solar Cells for Real: The Assembly Guide for Making Your Own Solar Cells. Solaronix, REV. 2012;3: 12.
23. Riaz R, Ali M, Maiyalagan T, Arbab AA, Anjuk AS, Lee S, Ko MJ, Jeong SH. Activated charcoal and reduced graphene sheets composite structure for highly electro-catalytically active counter electrode material and water treatment. *International Journal of Hydrogen Energy*. 2019: 1-13. Available from: doi.org/10.1016/j.ijhydene.2019.06.138.
24. Daniel LS, Nagai H, Yoshida N, Sato M. Photocatalytic Activity of Vis-Responsive Ag-Nanoparticles/TiO_2 Composite Thin Films Fabricated by Molecular Precursor Method (MPM). *Catalysts*. 2013;3(3): 625-645. Available from: doi: 10.3390/catal3030625.

25. Ghann W, Kang H, Sheikh T, Yadav S, Chavez-Gil T, Nesbitt F, Uddin J. Fabrication, Optimization and Characterization of Natural Dye Sensitized Solar Cell. *Sci. Rep*. 2017;7: 41470. Available from: doi: 10.1038/srep41470.
26. Arbab AA, Sun KC, Sahito IA, Memon AA, Choi YS, Jeong SH. Fabrication of textile fabric counter electrode using activated charcoal doped multi walled carbon nanotube hybrids for dye sensitized solar cells. *J. Mater. Chem. A*. 2016;4(4): 1495-1505. Available from: doi: 10.1039/c5ta08858e.
27. Arbab AA, Sun KC, Sahito IA, Qadir MB, Choi YS, Jeong SH. A novel activated-charcoal-doped multiwalled carbon nanotube hybrid for quasi-solid-state dye-sensitized solar cell outperforming Pt electrode. *ACS App. Mater. Interfaces*. 2016;8(11): 7471-7482.
28. Pramono SH, Maulana E, Prayogo AF, Djatmika R. Characterization of dye-sensitized solar cell (DSSC) based on chlorophyll dye. *International Journal of Applied Engineering Research*. 2015;10(1): 193-205.
29. Memon AA, Arbab AA, Sahito IA, Sun KC, Mengal N, Jeong SH. Synthesis of highly photo-catalytic and electro-catalytic active textile structured carbon electrode and its application in DSSCs. *Solar Energy*. 2017;150: 521-531. Available from: http://dx.doi.org/10.1016/j.solener.2017.04.052.
30. Selvaraj P, Roy A, Ullah H, Sujatha Devi P, Tahir AA, Mallick TK, Sundaram S. Soft-template synthesis of high surface area mesoporous titanium dioxide for dye-sensitized solar cells. *Int. J. Energy Res*. 2019;43(1): 523-534. Available from: doi: 10.1002/er.4288.
31. Alhamed M, Issa AS, Doubal AW. Studying of natural dyes properties as photo-sensitizer for dye sensitized solar cells (DSSC). Journal of electron Devices. 2012;16(11): 1370-1383.

32. Wang XF, Kitao O. Natural chlorophyll-related porphyrins and chlorins for dye-sensitized solar cells. *Molecules*. 2012;17(4): 4484-4497.
33. Syafinar R, Gomesh N, Irwanto M, Fareq M, Irwan YM. Chlorophyll pigments as nature-based dye for dye-sensitized solar cell (DSSC). *Energy Procedia*. 2015;79: 896-902. Available from: doi: 10.1016/j.egypro.2015.11.584.
34. Sun KC, Memon AA, Arbab AA, Sahito IA, Kim MS, Yeo SY, Choi YO, Kim YS, Jeong SH. Electrocatalytic porous nanocomposite of graphite nanoplatelets anchored with exfoliated activated carbon filler as counter electrode for dye sensitized solar cells. Solar Energy. 2018;167: 95-101.
35. Calogero G, Citro I, Di Marco G, Minicante SA, Morabito M, Genovese G. Brown seaweed pigment as a dye source for photoelectrochemical solar cells. Spectrochimica Acta Part A: Molecular and Biomolecular Spectroscopy. 2014;117: 702-706.
36. Godibo DJ, Anshebo ST, Anshebo TY. Dye sensitized solar cells using natural pigments from five plants and quasi-solid state electrolyte. Journal of the Brazilian Chemical Society. 2015;26(1): 92-101.
37. Arof AK, Ping TL. Chlorophyll as Photosensitizer in Dye-Sensitized Solar Cells. Chlorophyll. 2017: 105.
38. Eli D, Musa GP, Ezra D. Chlorophyll and betalain as light-harvesting pigments for nanostructured TiO_2 based dye-sensitized solar cells. Journal of Energy & Natural Resources. 2016;5(5): 53-58.
39. Shah S, Buraidah MH, Teo LP, Careem MA, Arof AK. Dye-sensitized solar cells with sequentially deposited anthocyanin and chlorophyll dye as sensitizers. Optical and Quantum Electronics. 2016;48(3): 219.

40. Shanmugam V, Manoharan S, Sharafali A, Anandan S, Murugan R. Green grasses as light harvesters in dye sensitized solar cells. Spectrochimica Acta Part A: Molecular and Biomolecular Spectroscopy. 2015;135: 947-952.

41. Atkins P, Overton T, Rourke J, Weller M, Armstrong F, Hagerman M. Shriver & Atkins' Inorganic Chemistry. 5th ed. New York: W. H. Freeman and Company; 2010.

42. Robinson JW, Frame EMS, Frame II GM. Undergraduate instrumental analysis. 7th ed. 2014.

43. Skoog DA, Holler FJ, Crouch SR. Principles of Instrumental Analysis. 6th ed. Canada: David Harris; 2007.

44. Harris DC. Quantitative chemical analysis. 8th ed. United States of America. Clancy Marshall; 2010.

45. Edaq. Echem Manual. 1999.

46. Ohno T, Sarukawa K, Tokieda K, Matsumura M. Morphology of a TiO_2 Photocatalyst (Degussa, P-25) Consisting of Anatase and Rutile Crystalline Phases. *J Catalysis.* 2001; 203: 82-86.

47. Thiruvenkatachari R, Vigneswaran S, Moon IS. A review on UV/TiO_2 photocatalytic oxidation process. *Korean J. Chem. Eng*. 2008; 25(1): 64-72.

48. Ohtani B, Prieto-Mahaney OO, Li D, Abe R. What is Degussa (Evonik) P25? Crystalline composition analysis, reconstruction from isolated pure particles and photocatalytic activity test.

49. Hurum DC, Agrios AG, Gray KA, Rajh T, Thurnauer MC. Explaining the Enhanced Photocatalytic Activity of Degussa P25 Mixed-Phase TiO_2 Using EPR. *J. Phys. Chem. B*. 2003; 107: 4545-4549.

50. Raihana M. Performance analysis of Graphite and Multi Wall Carbon Nanotube based Counter Electrodes in Dye Sensitized Solar Cells, *University of Dhaka*. M. Sc. Thesis, 2016.
51. Kalipi M. Performance enhancement of Ag-NP/TiO_2 using Chlorophyll as dye sensitizer, *University of Namibia*. M. Sc. Thesis, 2019.